

10/12/11

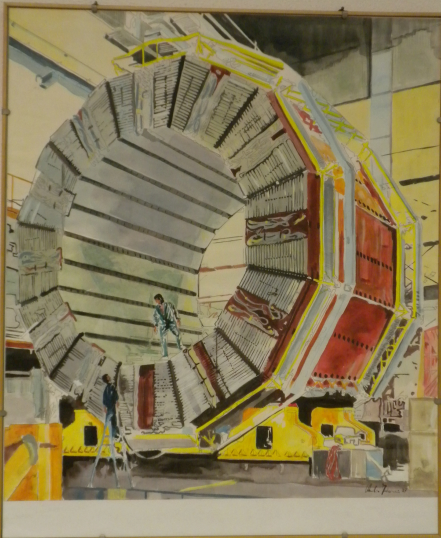
Detectors at Tevatron and LHC: selective review

Pawel de Barbaro,
University of Rochester

Stori'11
Frascati, Oct 10 - 14, 2011

Thanks to Willis Sakumoto and Gino Bolla (CDF/CMS)
and Sasha Solodkov (ATLAS)

P. de Barbaro, U. of Rochester

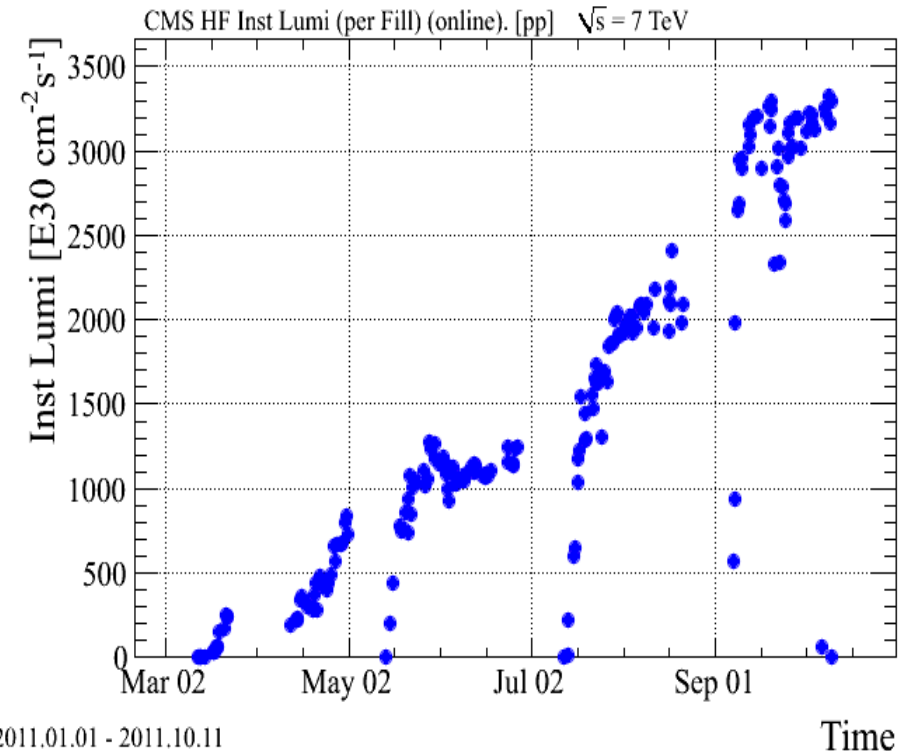
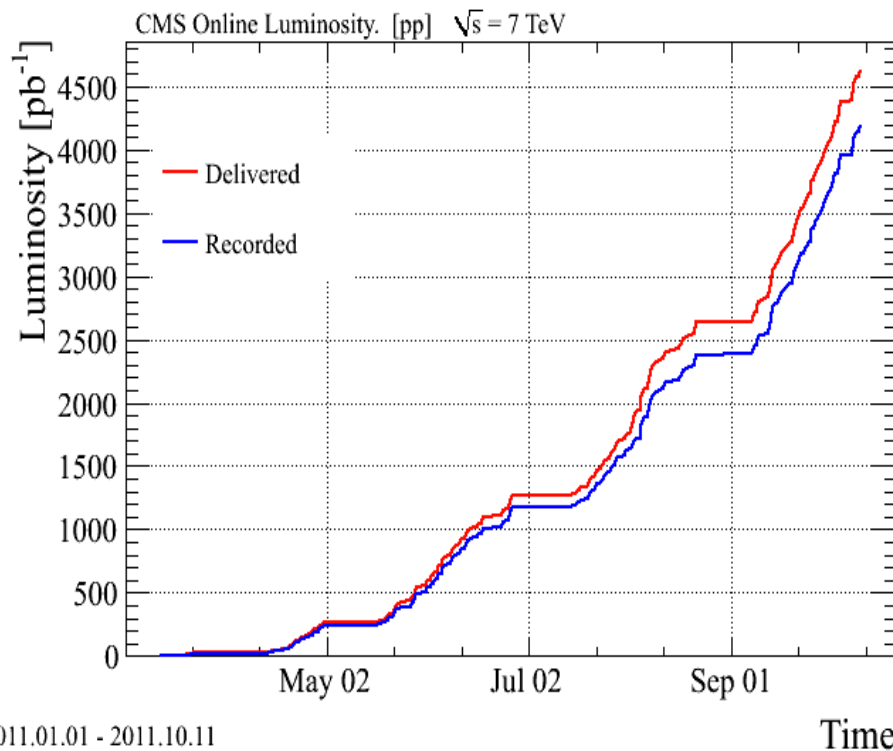


Passing the baton

- After twenty years of very successful operation, Tevatron program at Fermilab has been terminated
- Two collider experiments, CDF and D0, collected over 10 fb^{-1} of data each.
- Over the years, these well understood detectors gave us beautiful results, including discoveries and measurements in electroweak, top quark and heavy flavor physics, Higgs and Beyond Standard Model searches
- On other side of the ocean, LHC program at CERN, just in its second year of operation, has reached $3 \cdot 10^{33} \text{ cm}^{-2}/\text{s}$ of instantaneous luminosity.
- By end of this month, more than 5 fb^{-1} of pp collisions at 7 TeV center-of-mass energy will be collected by CMS and ATLAS experiments



- We have all witnessed amazing performance of LHC in 2010 and its even more amazing performance in 2011
- It is interesting to take a critical look at performance of LHC detectors and compare our pre-collision expectations with operational realities.



Delivered Integrated luminosity in 2011 $> 4.5 \text{ fb}^{-1}$

Peak Instantaneous luminosity: $> 3 \cdot 10^{33} \text{ cm}^{-2}/\text{s}$



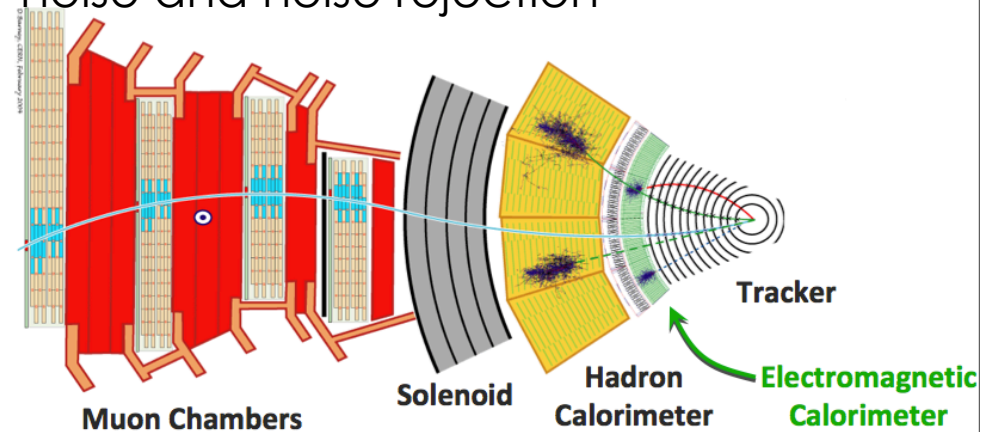
P. de Barbaro, U. of Rochester

overview

4

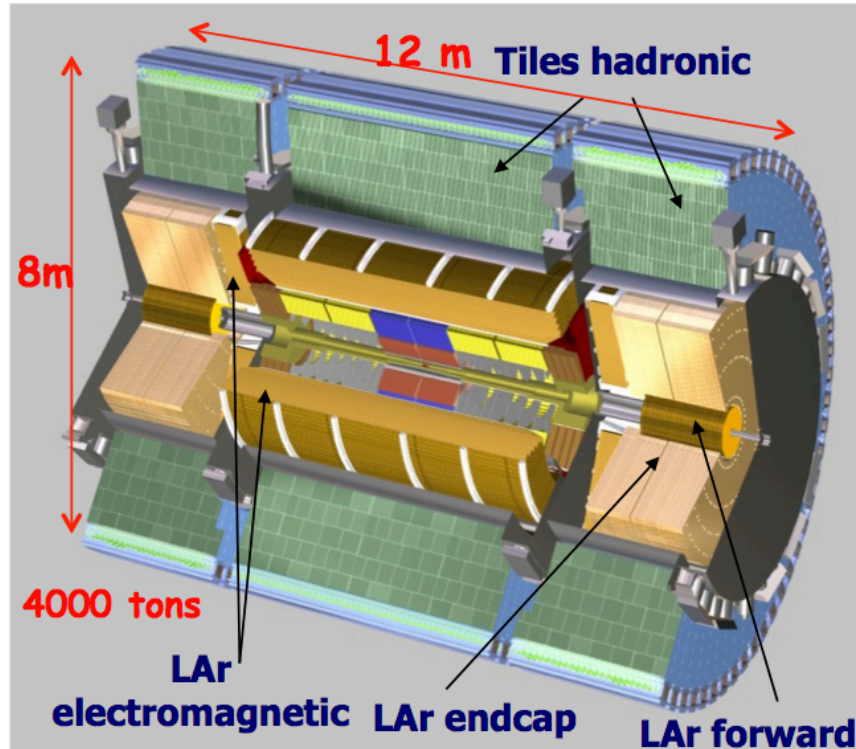
- Compare detector systems
- Focus on EM and Hadron Calorimeters
- Some comments on Si Tracker
- Challenging issues:

stability of response
sensitivity to radiation
high pile-up
noise and noise rejection



ATLAS calorimeters: Liquid Argon and TileCal

5



Hadron calorimeter

Trigger; measure jets; $E_{T,miss}$:

- $\sigma/E \sim 50-60\%/\sqrt{E} \oplus 3\%$ central
- $\sigma/E \sim 90\%/\sqrt{E} \oplus 7\%$ in fwd
- $\sigma(E_{T,miss}) / \Sigma E_T \approx 55\%$

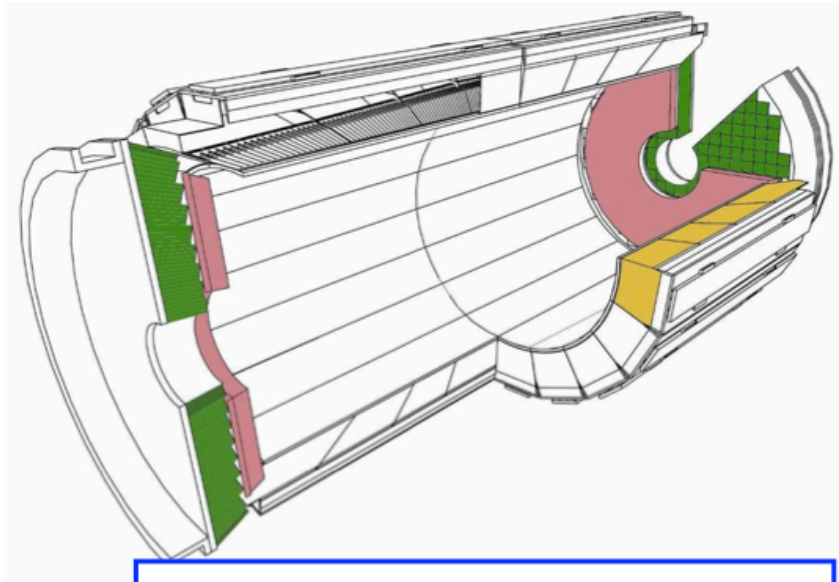
- $|\eta| < 1.7$: Fe/scint. Tiles (Tilecal)
- $3.2 < |\eta| < 1.5$: Cu-Lar (HEC)
- $3.1 < |\eta| < 4.9$: FCAL Cu/W-Lar

- $|\eta| < 4.9$
- 10λ at $|\eta|=0$
- $\Delta\eta \times \Delta\phi$: 0.1×0.1 up to $|\eta| < 2.5$
- 3-4 Longitudinal layers
- 20×10^3 channels

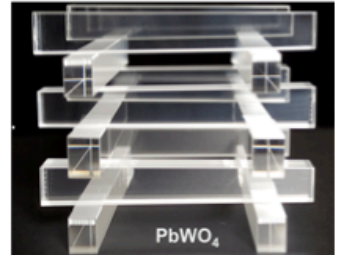
Lar-Pb EM calorimeter ($|\eta| < 3.2$):

- e/ γ trigger, identification; measurement
- $\sigma/E \sim 10\%/\sqrt{E} \oplus 0.7\%$
- Granularity: 0.025×0.025 ; $22X_0$
- 3 long. layers + presampler ($0 < |\eta| < 1.8$)
- 180×10^3 channels

CMS ECAL calorimeter



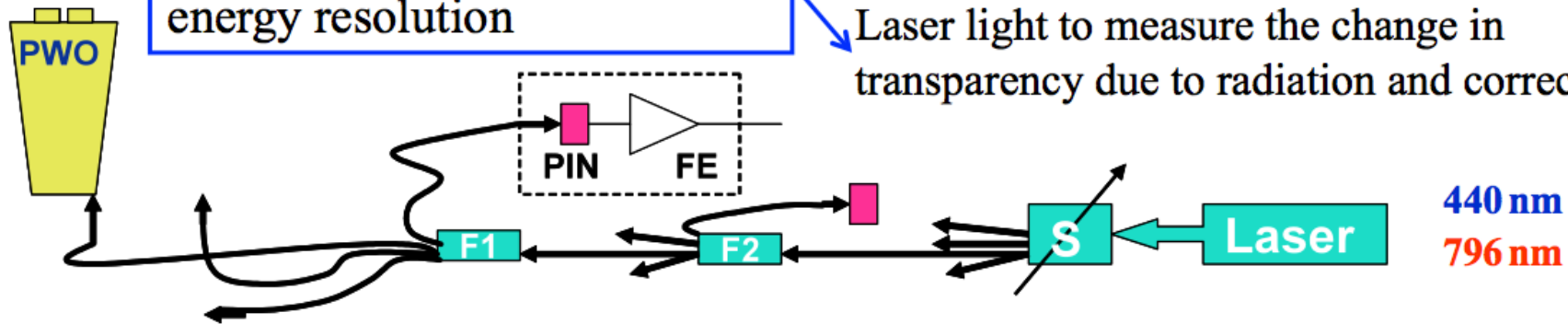
PbWO₄ crystals (~25 X₀)
 Photodetectors: APD, VPT
 Barrel: $|\eta| < 1.48$ 61200 ch
 Endcap: $1.48 < |\eta| < 3$ 14648 ch



Preshower: $1.65 < |\eta| < 2.6$
 two layers of Pb absorber and
 Si strips 1.98x63 mm² x-y view

needed to achieve excellent energy resolution

monitor temperature and HV stability
 Laser light to measure the change in transparency due to radiation and correct for it



CMS ECAL: Test Beam results



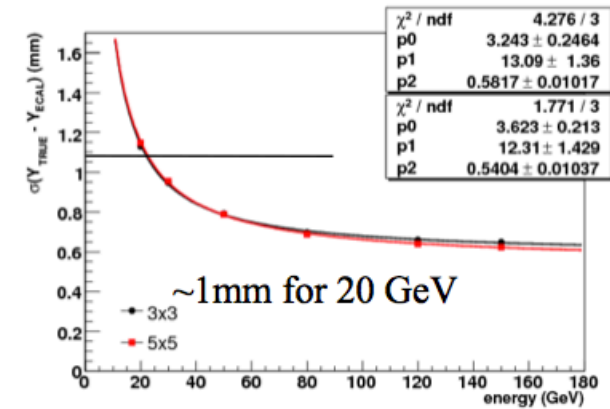
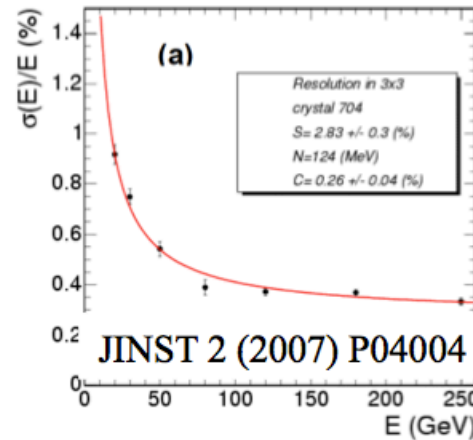
Extended studied of barrel ECAL modules with electron and pion beams

Study:

Position resolution

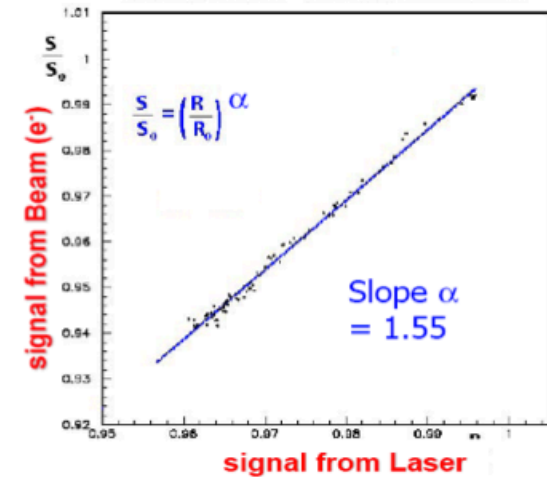
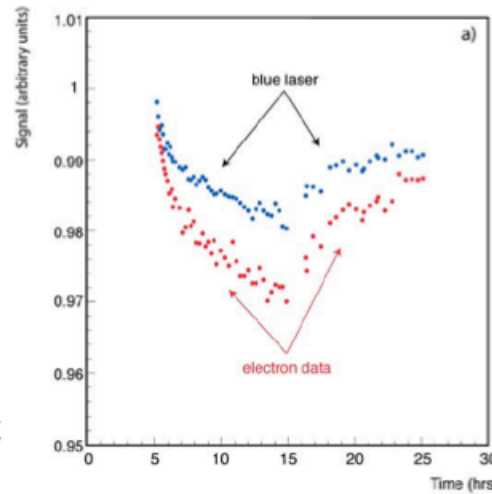
Energy resolution

$$\frac{\sigma}{E} = \frac{2.8\%}{\sqrt{E}} \oplus \frac{0.125}{E} \oplus 0.3\%$$



Monitor the response to laser light and electrons during irradiation and recovery

S: response to electrons $\frac{S}{S_0} = \left(\frac{R}{R_0} \right)^\alpha$ R: response to laser light



CMS ECAL in-situ calibration

8

Calibration with:

Φ symmetry

π^0 mass peak



Combining with pre-calibration the resulting precision is better than 0.5% in most of the barrel and about 2% in the endcap

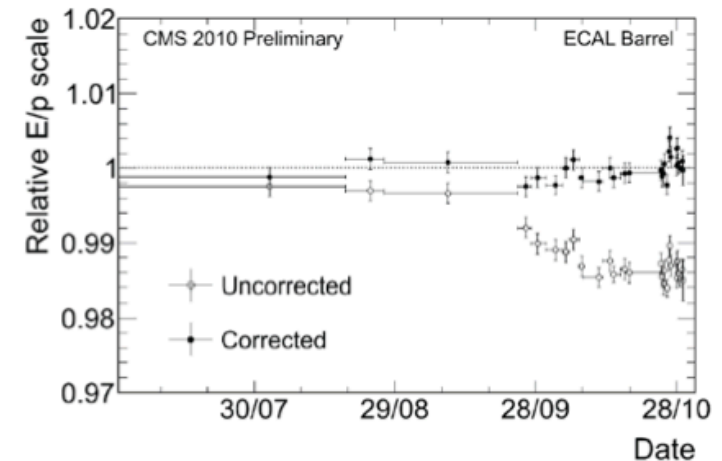
CMS EGM-10-003

$$E_{e,\gamma} = F_{e,\gamma} \sum_i G \times S_i(t) \times C_i \times A_i$$

Average laser corrections are cross checked with π^0 and E/p of electron from W

Energy scale is set with the Z peak in the ee mass distribution

Comparison with MC is used to extract the resolution



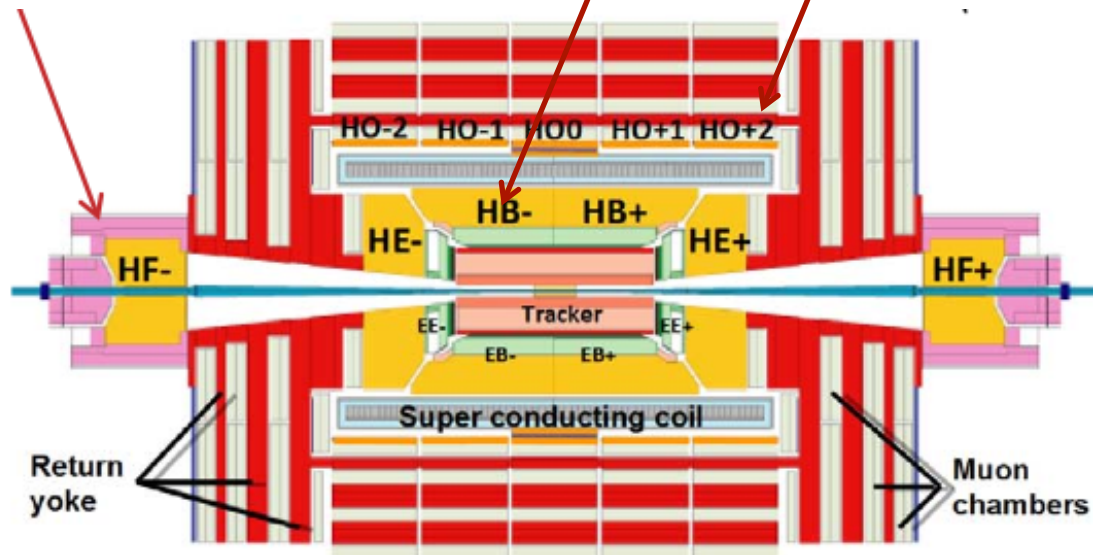
CMS Hadron Calorimeter

- * Barrel and Endcap, (HBHE):
sampling scintillator/brass calorimeter
- * Readout: Hybrid Photo-detector (HPD),
operating Inside 3.8T magnet

Forward (HF) :
Cherenkov light from
scintillating quartz fiber in
steel absorber is read out
with conventional PMT

Outer (HO):

- Tail catcher with one (two in HO/ring0)
scintillator layers and HPD readout,
* Outside of solenoid



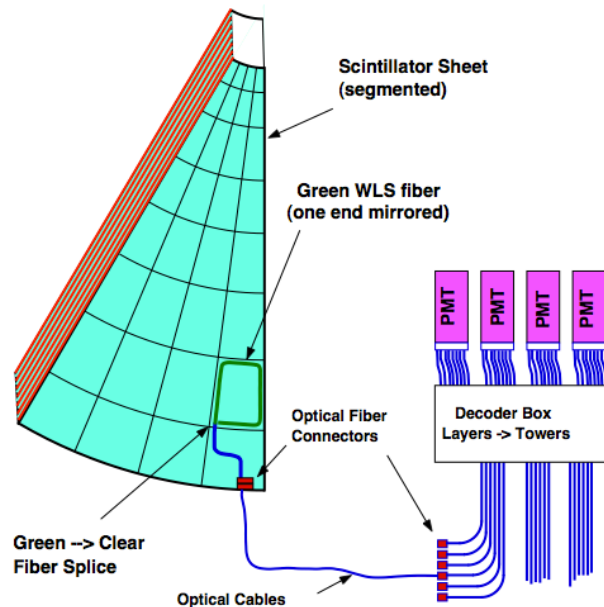
- > 500 days of practically un-interrupted operation
- 50 ns bunch spacing
- > 20 pile-up events per beam crossing

HCAL sub-detector very stable over 2010-11 period with
> 99% of HCAL channels live

CDF Plug Upgrade: Megatiles and sigma grooves

10

9. The PEM, PPR, and PHA consist of “megatiles” with tile/fiber readout

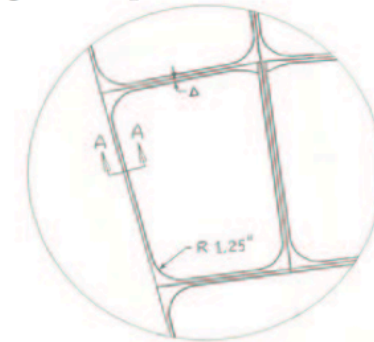


- Megatiles: 15° (PEM, PPR) or 30° (PHA) ϕ sector mechanical units that securely hold and protect scintillator tiles and its fragile fibers
- The Run II plug pioneered the megatile
- Fiber optics with mass termination connectors for ease of construction and assembly

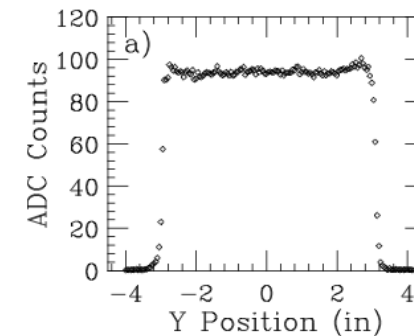
P. de Barbaro, U. of Rochester

10. Tile/fiber basics

- σ groove pattern developed by CDF



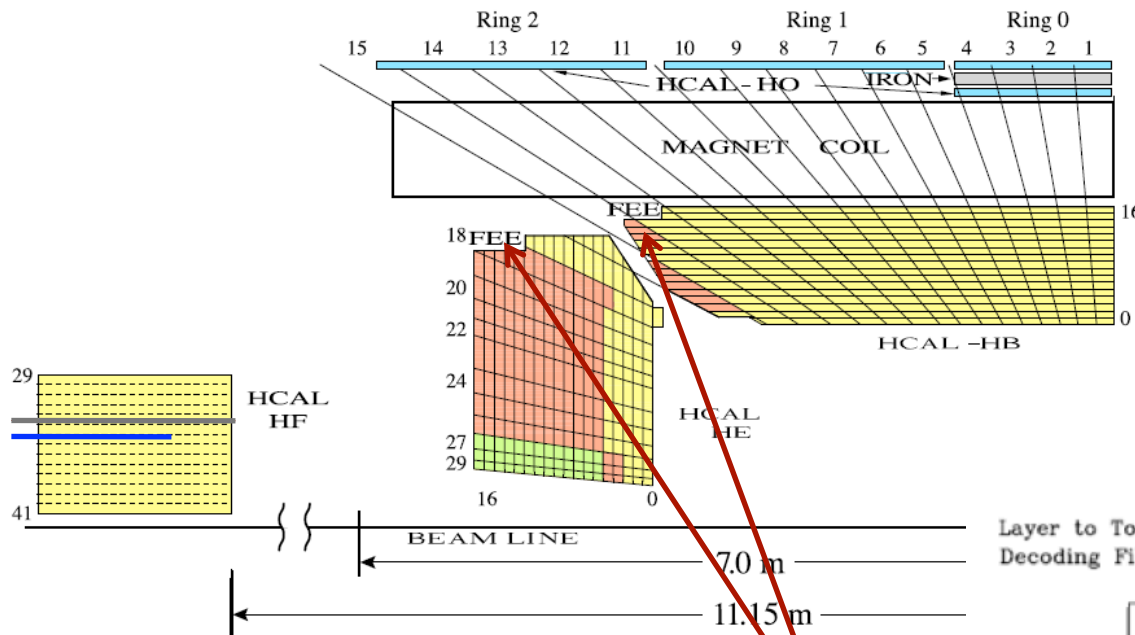
- Relatively flat transverse response



- Depth of fiber groove must be tuned
- Fiber groove close to tile edge
- Light yield \sim Length/Area
- PEM uniformity: $\sim 5\%$
- PHA uniformity: $\sim 2\%$

10/12/11

HCAL segmentation



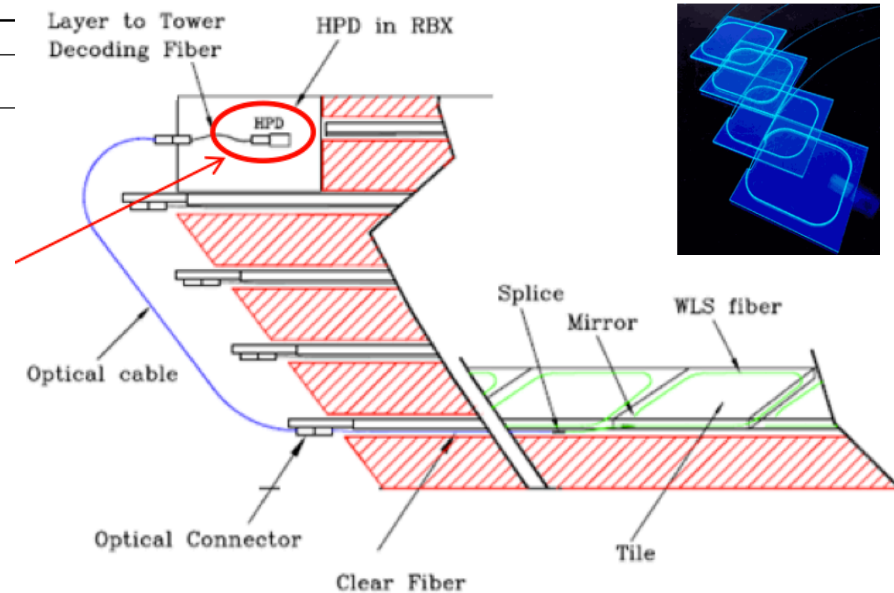
HB, HE, sampling calorimeter with plastic scintillator tiles and wave-length shifting (WLS) fiber in brass absorbers. Tail catcher outside the magnet (HO)

$\Delta\eta \times \Delta\phi = 0.087 \times 0.087$
 Barrel $0 < |\eta| < 1.4$
 Endcap $1.3 < |\eta| < 3.0$

Forward $2.9 < |\eta| < 5.0$
 $\Delta\eta \times \Delta\phi = 0.17/0.35 \times 0.17/0.35$

HPD

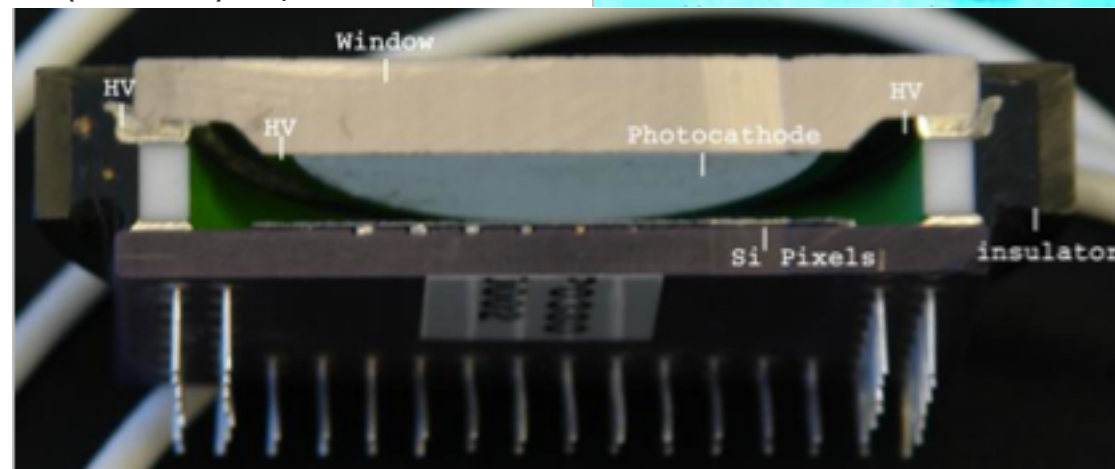
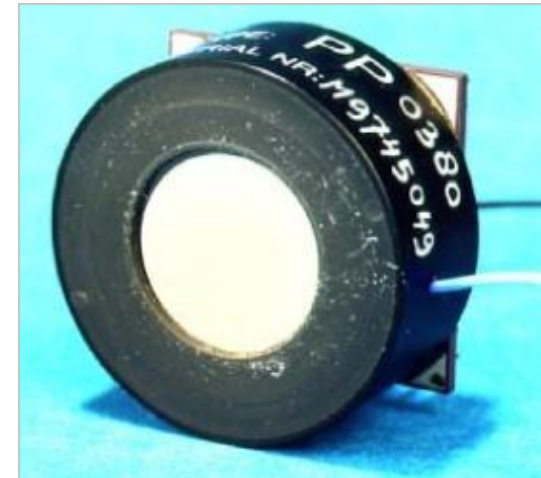
HPD: Hybrid photo-detector



Hybrid Photo-detectors

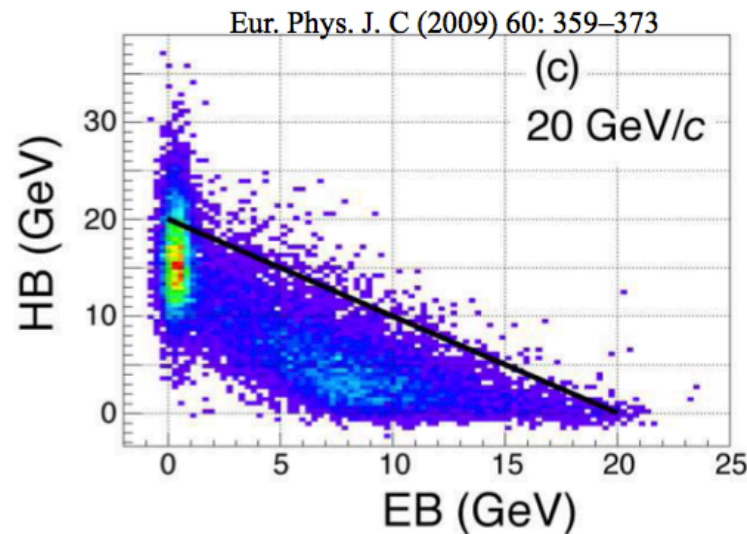
- Hybrid photo-detectors (HPDs) were designed to operate in high magnetic fields, up to 4 Tesla
- Proximity-focusing with 3.5mm gap, with E field parallel to B field
- HV of 8kV with 18 pixels (20mm² each)
- Gain of ~ 2k, linear response over large dynamic range from min-ionizing particles (muons) up to 3 TeV hadron showers

* 2008 JINST 3 S08004
* P. Cushman et al.,
NIM A 504 (2003) 502



CMS calorimeter combined response: Test Beam results

13



Ecal+Hcal is a non compensating calorimeter with $e/h \sim 1.4$



Non linearity and contribution to energy resolution.

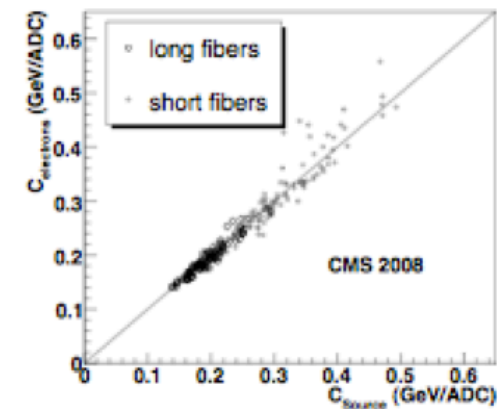
50 GeV/c π (MIP in ECAL) are chosen as reference for calibration.

Calibration of all HCAL tiles with γ source (^{60}Co)



comparison with TB demonstrates a 5% precision.

For HF the precision is better than 12%



CMS HCAL: Calibration methods

14

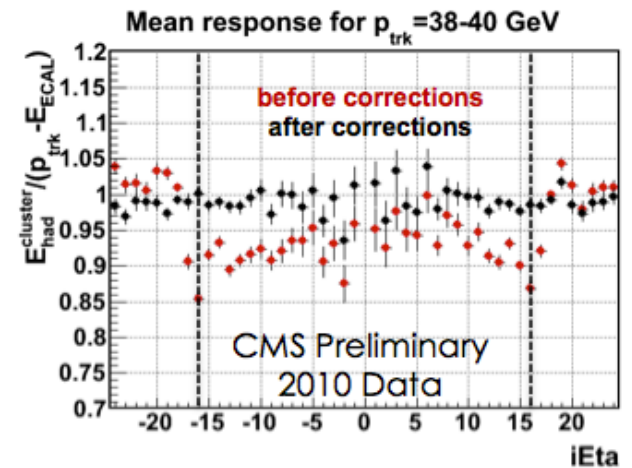
- Prior to LHC start-up, initial calibration of HCAL
 - Charge injection calibration (fC/ADC) as part of incoming QC only
(on-the-bench measurements)
 - Co⁶⁰ radio-active sources (after assembly in the surface hall, 2006/07) and cosmic ray muons in the underground hall
 - Absolute energy scale determined with pion and electrons test beams
(on selected wedges) and carried over using radioactive sources

- At the start-up of LHC, additional calibration was performed with Splash events (proton bunches hitting collimators upstream of CMS resulting in large horizontal flux of muons traversing CMS detectors)

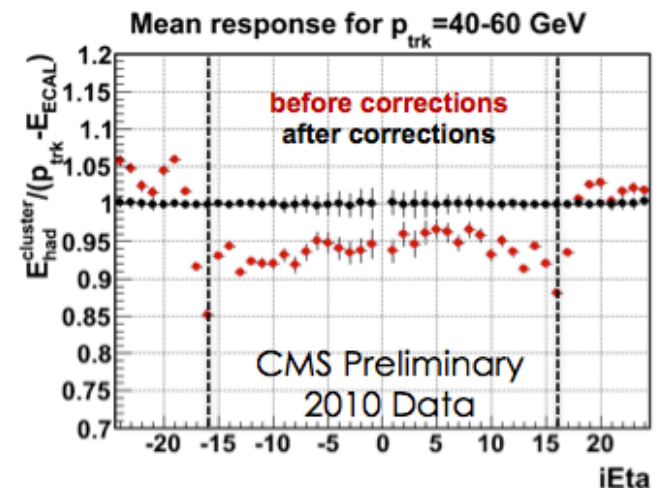
- Monitoring of HPD and PMT response (at the hardware level):
 - Stability of photo-detector gains is monitored using LED system
 - Data is recorded during calibration sessions (periods between LHC fills)
 - Pedestals and signal synchronization (timing) is monitored using Laser data
 - Data is recorded using triggers generated during LHC orbit abort gap (no proton bunches)

- Collisions data (2010 and 2011) allows to obtain calorimeter response corrections, which include both Phi-symmetry and isolated hadrons methods

Check method using lower p_{trk} tracks

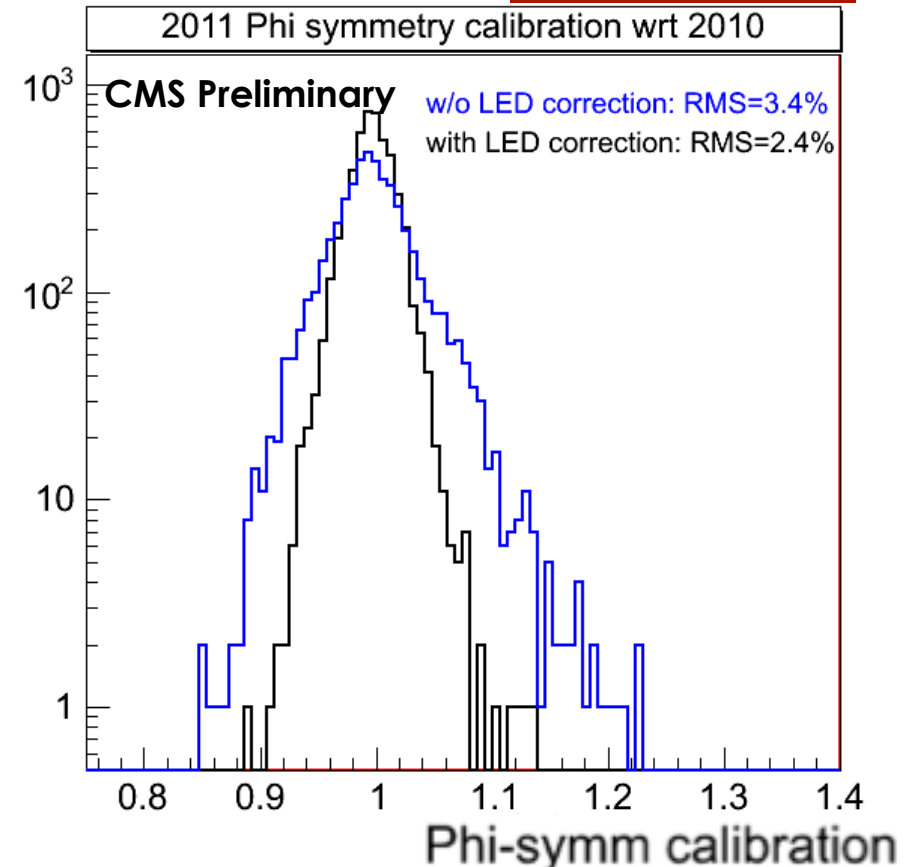
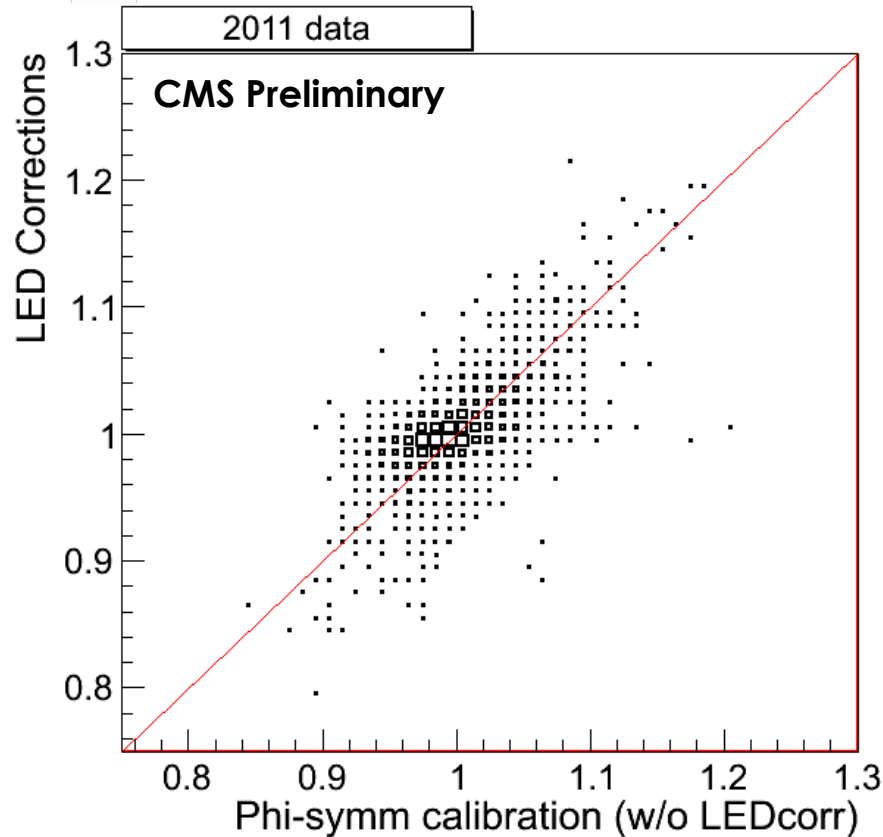


Derive corrections using $p_{trk} = 40-60$ GeV



Phi-Symmetry Calibration (2011)

15



Gain corrections are based on monitoring of response of HPDs to LED signals.
Phi-symmetry corrections are calculated w/o and with LED gain corrections.

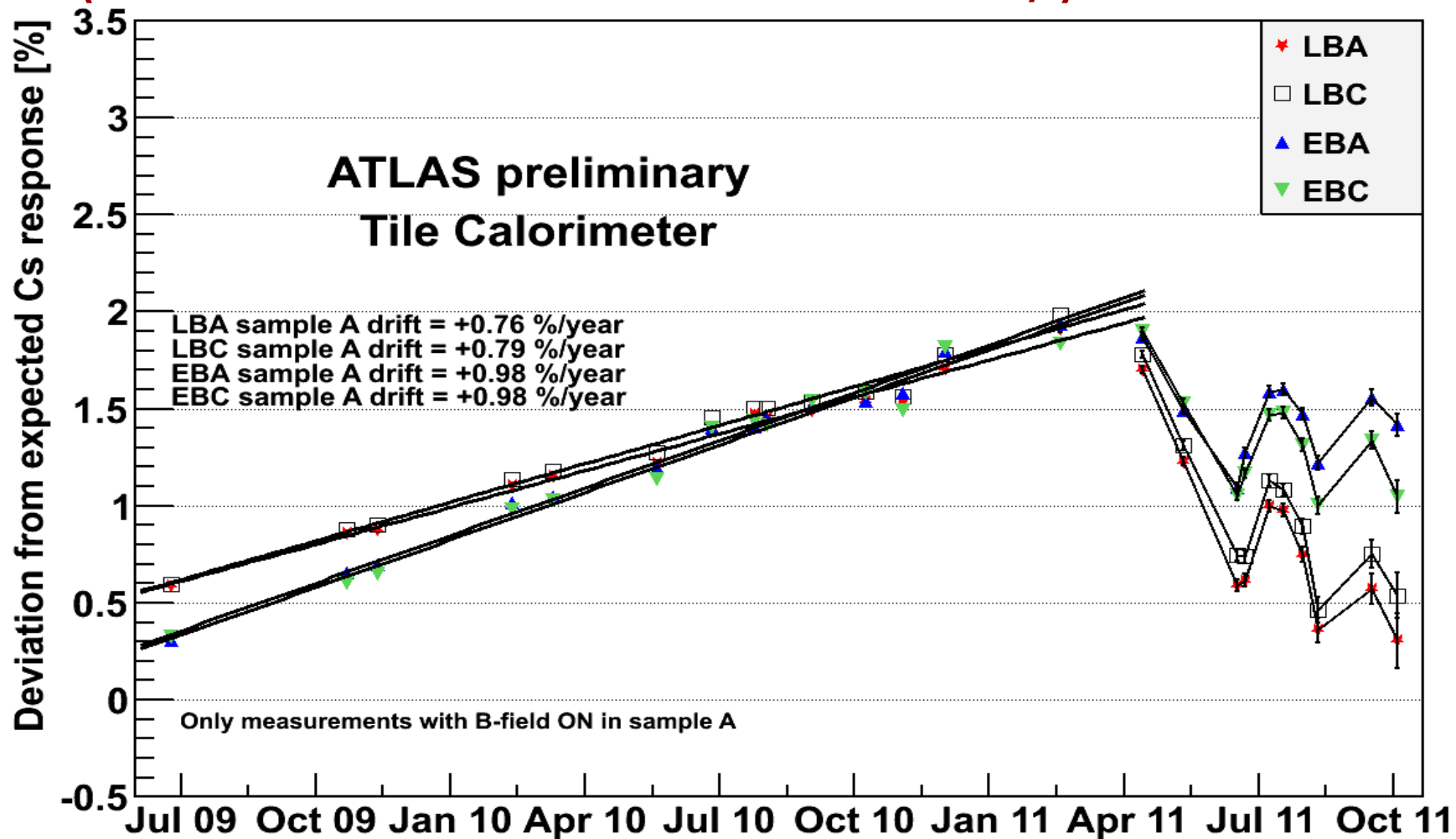
Conservative estimate of error on phi-symmetry calibration is 1.5%.

Paola de Barbaro, U. of Rochester

LED corrections reduce spread of 2011 phi-symmetry calibration wrt 2010 results

10/12/11

ATLAS: Cs source calibrations (corrected for source decay)



Noise in HBHE (HPD readout)

- The backgrounds in HB and HE are almost entirely dominated by electronics effects, causing triggers with randomly overlap with collision physics triggers
- Rates are practically constant (as a function of luminosity) and independent of collisions. Overlap with physics is low (1 per 10^5).
- Trigger rates and contamination is an issue for high ET and high MET
- development of efficient noise filtering at High Level Trigger (HLT) and offline reconstruction is very important
 - HPD/RBX noise produce distinct patterns in HCAL
 - Filters have been developed making use of hit patterns, timing, pulse shape, and EM fraction

Origins of HPD and RBX noise

HPD Ion Feedback (*~1 HPD channel*)

Photoelectron induced liberation of ions from the silicon diode which accelerate across the HV gap and interact with the photocathode freeing additional photoelectrons

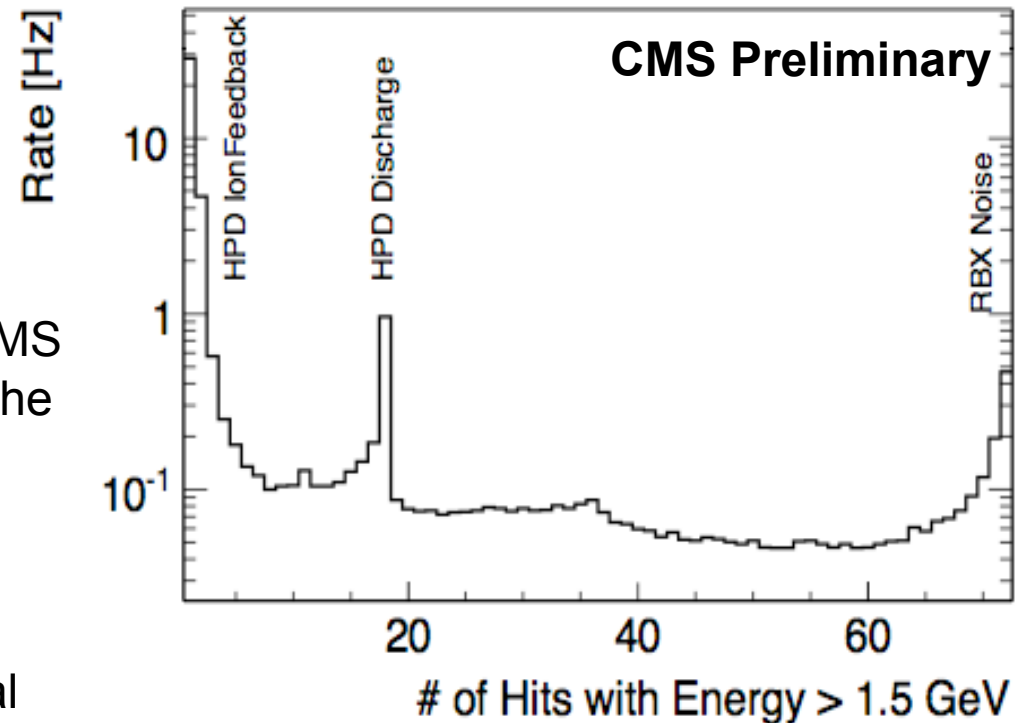
HPD Discharge (*up to 18 HPD channels*)

With the HPD operating at $\sim 8\text{kV}$ in the CMS magnetic field, dielectric flashover from the wall can produce large signals in many channels

RBX Noise (*up to 72 channels*)

Source unknown, possibly due to external noise coupling to HV of many channels across the whole RBX

CRAFT '09 Data, $E_{\text{RBX}} > 10 \text{ GeV}$



Readout Box (RBX) contains 4 HPDs,
With total of 72 readout channels

Anomalous signals in HF

19

Anomalous signals are event related

The probability per event depends on the energy pointing into HF

different contributing effects have been identified and addressed

- In time or early narrow signal: Cerenkov light from particles going through PMT window
- Mostly involve only one channel (Long OR Short fibers)
- Typical energy of signal 100-200 GeV
- HF timing: “window interactions” largely placed in BX-1, with calorimeter signal in BX
- Late/wide signals, originating from scintillating material in light guides between fibers or in PMTs



Anomalous signal Filtering in HF

20

HF Topological Filter (HLT)

Without filtering, the MET rate is too high to include HF in the triggers

Adding HF (with filtering) reduces MET100 by a further factor ~ 2 compared to no HF

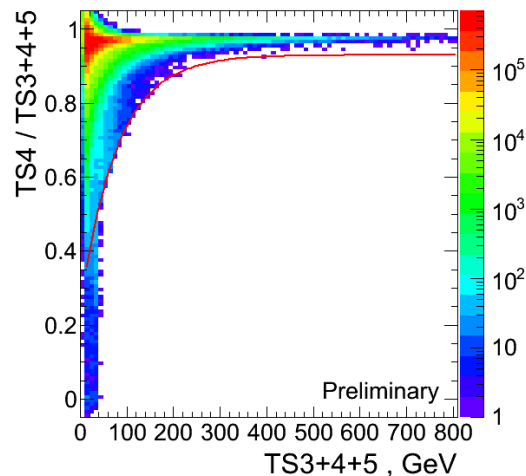
HF Pulse Shape Filter (HLT and Offline)

The ADC output of each channel is computed every 25 ns. HCAL records the ADC outputs from each channel for up to ten consecutive 25 ns intervals (“Time Slices”: TS), and the beam crossing occurs in TS4

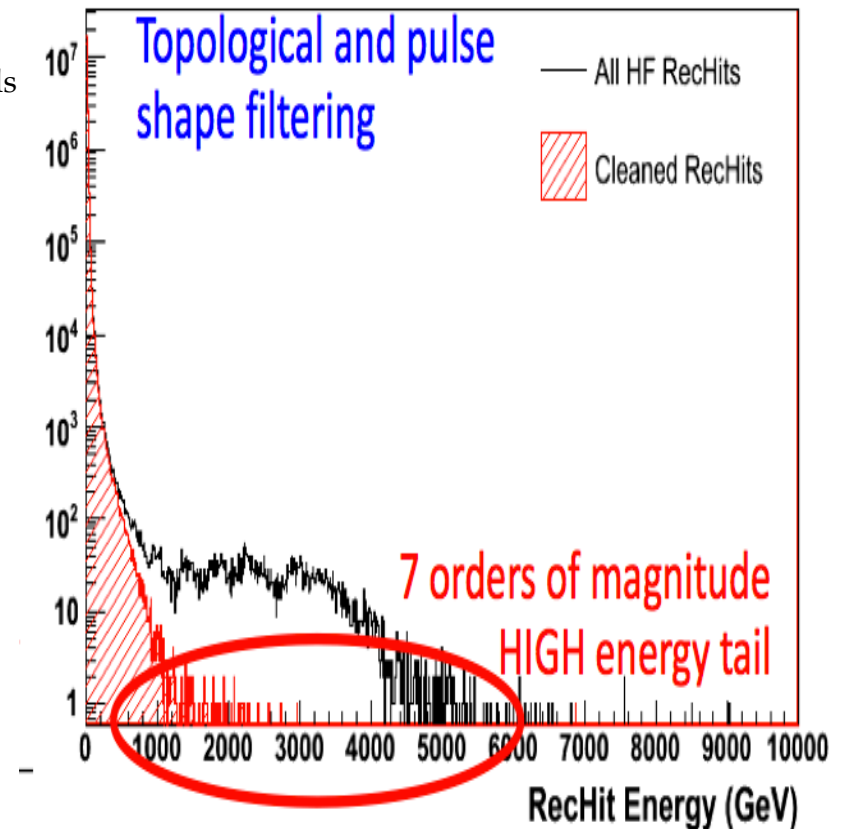
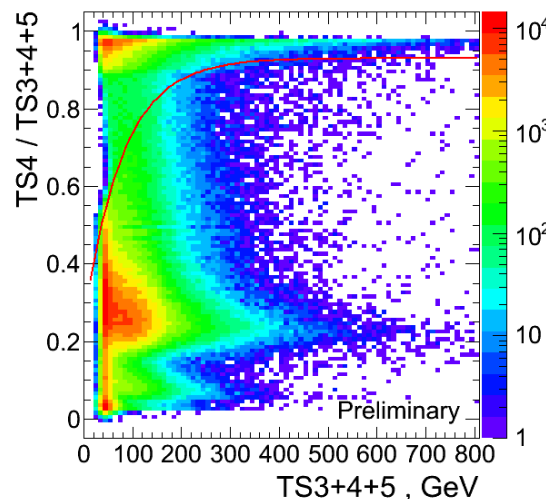
$$\text{HF Energy} = \text{TS4} + \text{TS5}$$

$$\text{Pulse Shape} = \text{TS4} / (\text{TS3} + \text{TS4} + \text{TS5})$$

Signal



Noise



The silicon detectors of the LHC

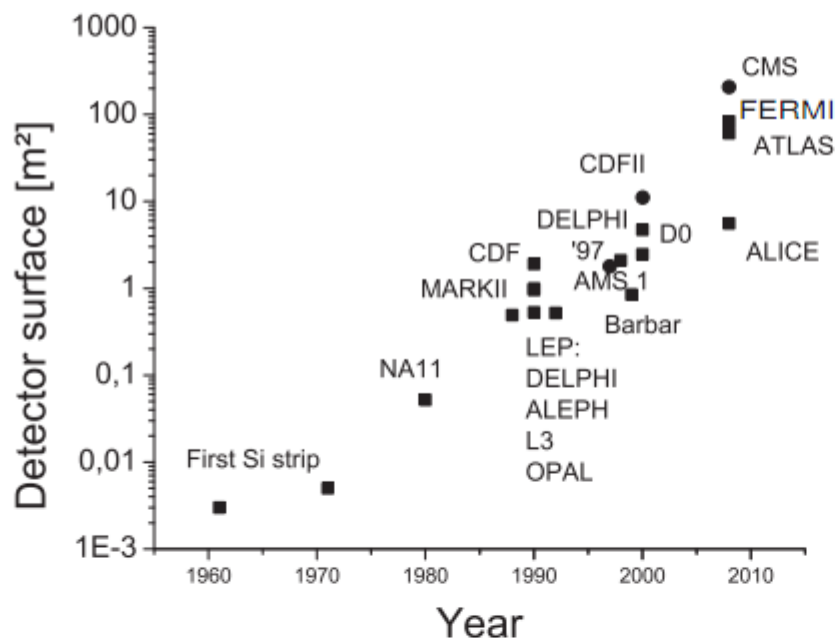


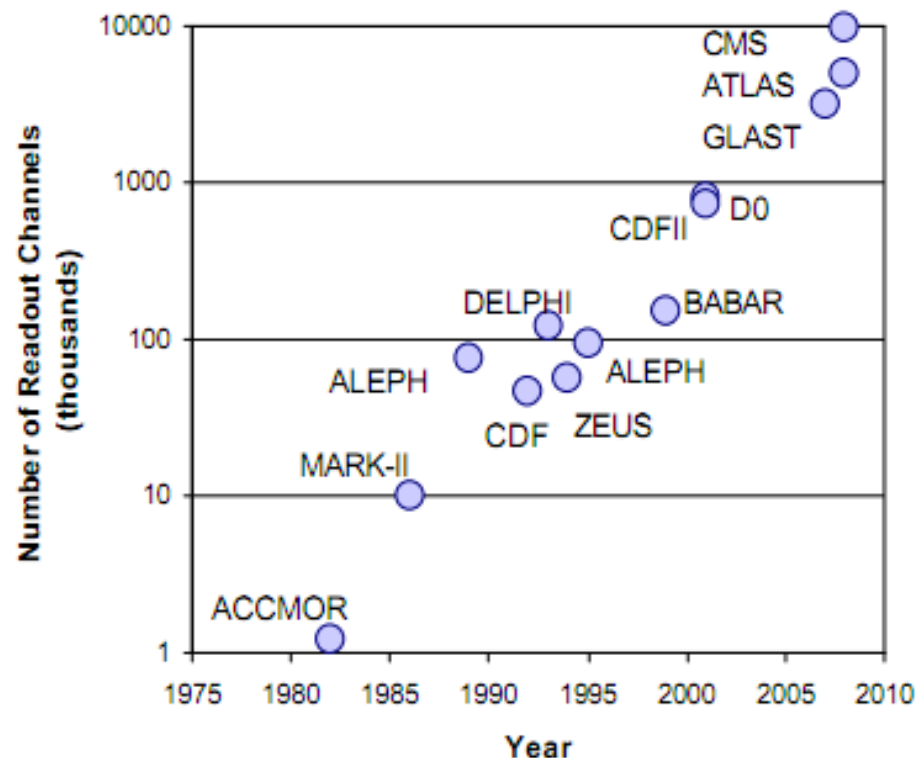
Figure 1: The evolution and usage of silicon as high energy physics detectors can be impressively shown by the increase in area during the last decades. [1]

On the plot on the right only strips channels are counted. The CMS/ATLAS pixel detectors add another 60-100 Million channels to what is shown

P. de Barbaro, U. of Rochester

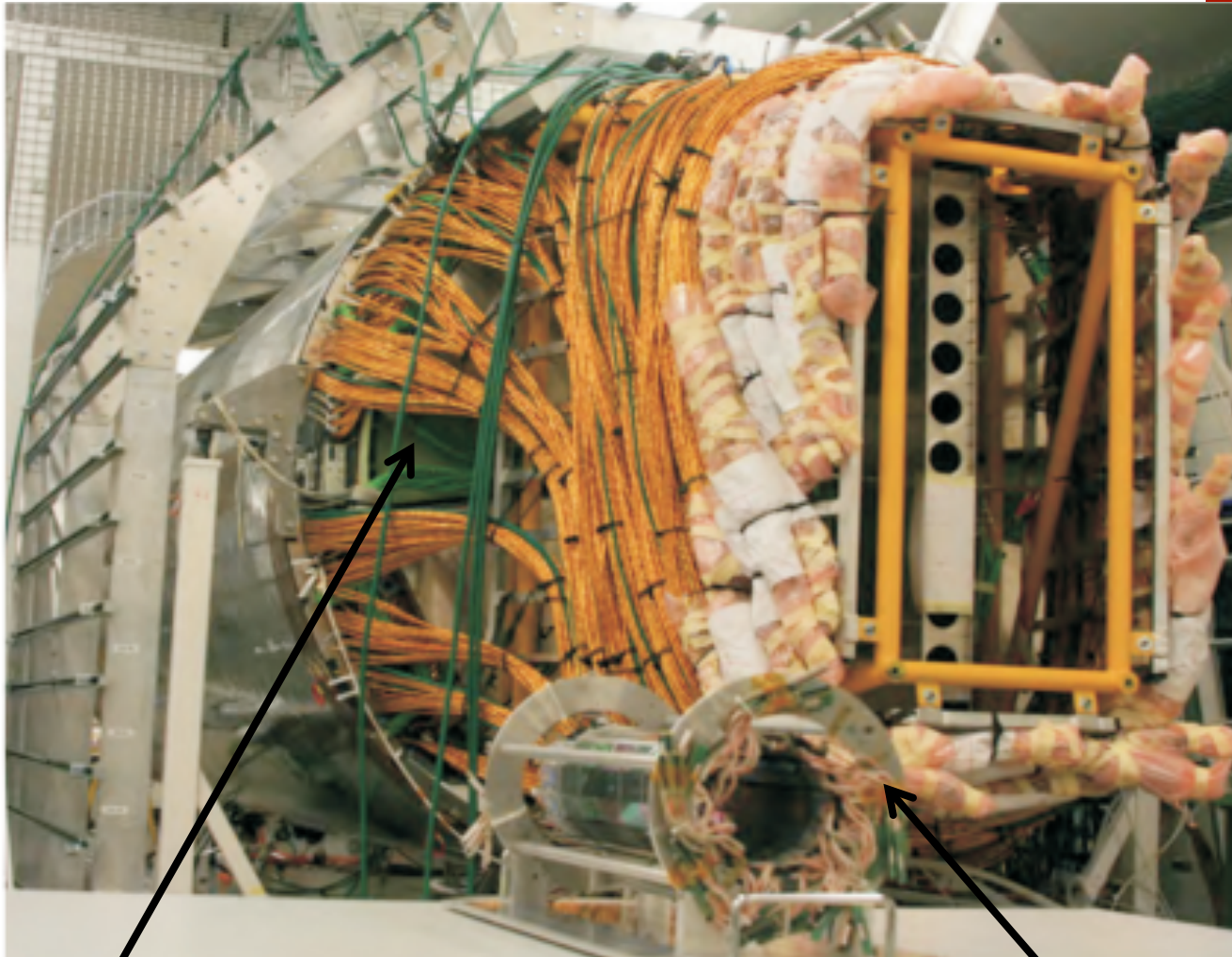
more than one order of magnitude bigger than the ones used at the Tevatron.

Up to 250 m² of silicon in CMS



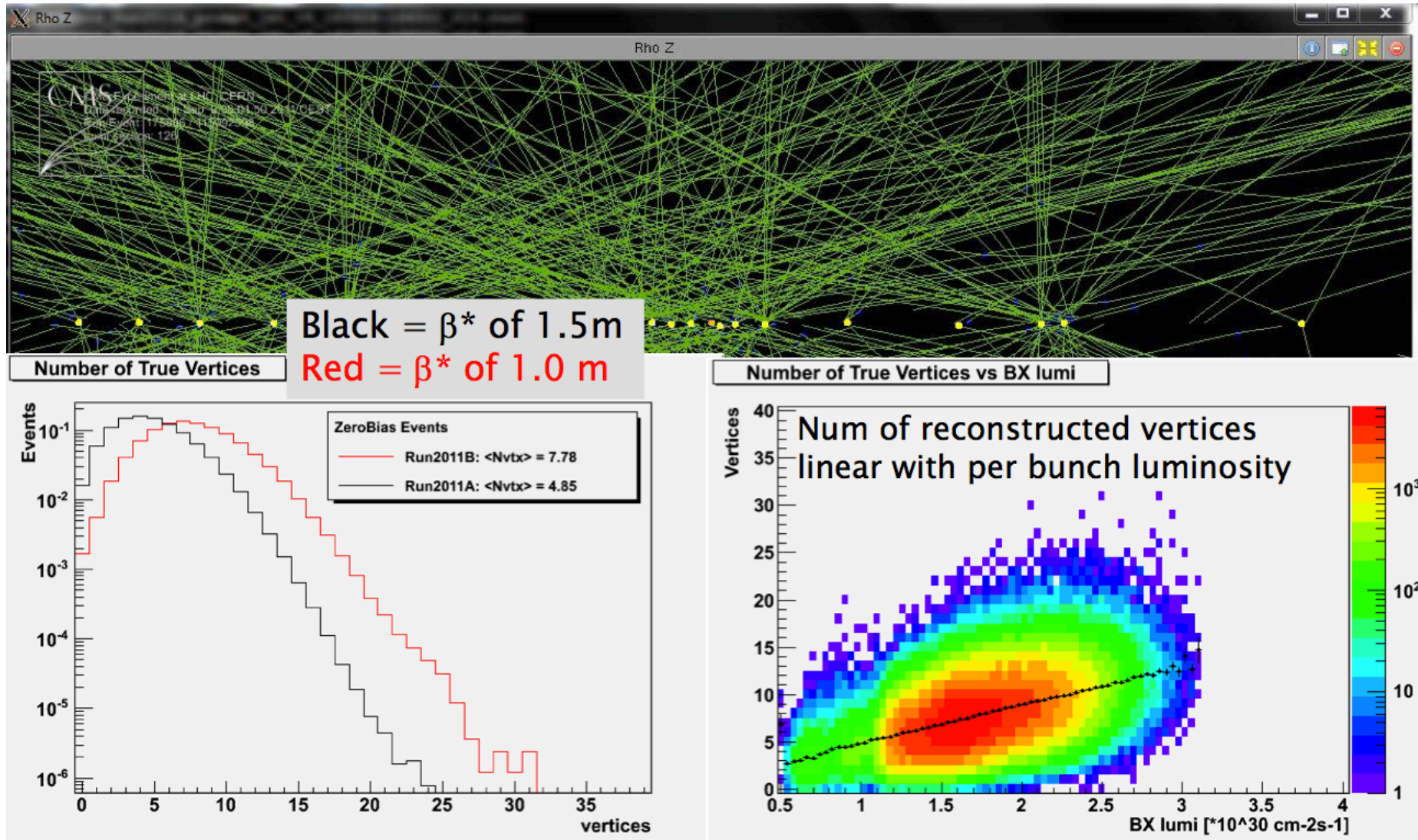
Silicon detectors: CMS and OPAL

22



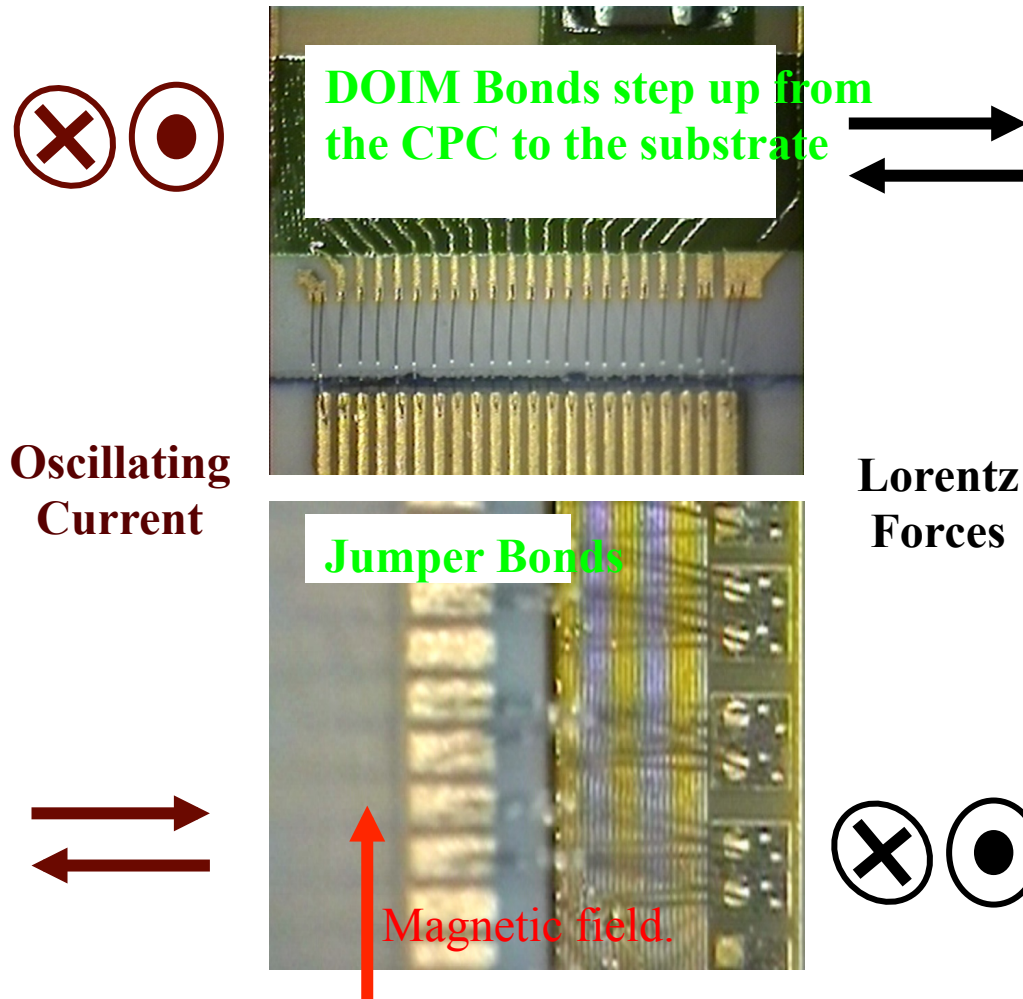
the packed CMS detector (before installation) vs the OPAL silicon tracker

CMS: tracking at hi pile-up





Wire-bonds in a magnetic field



- With a 1.4 T magnetic field, > 20 mA of current and a 2 millimeter bond in a plane that is orthogonal to the field the forces are in the range of $5e^{-4}$ N (50 mg).
- The induced movement should not exceed 3-4 μ m (hard to measure on a 25 μ m Al wire)
- Resonant behavior is expected and the natural resonant frequencies are in the kHz range depending on the length and shape of the wires (CDF is interested only up to 50 kHz)

Wire-bonds in B field: consequences for CMS

25

- ✓ All critical wire-bonds were encapsulated at the heel to dump the vibrations.

- ✓ Implementation of a “Trigger Inhibit” on potential resonances (triggers with fixed intervals)
 - Count time between readout commands (Δt_i)
 - If $(\Delta t_i - \Delta t_{i+1}) < 1\mu\text{sec}$ C++
 - If $C > 10$ pull the brakes and stop the trigger for a certain time window

- Add random trigger to the menu in case the beam conditions are resonant by nature (single bunch in the LHC)

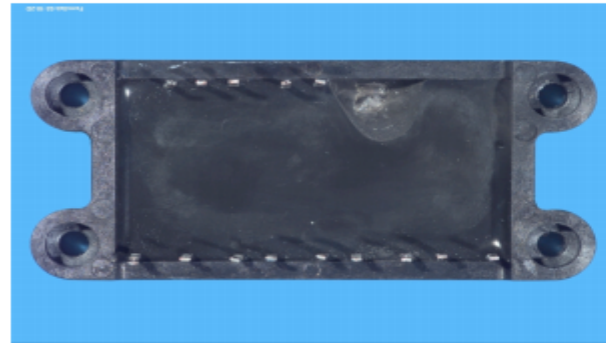
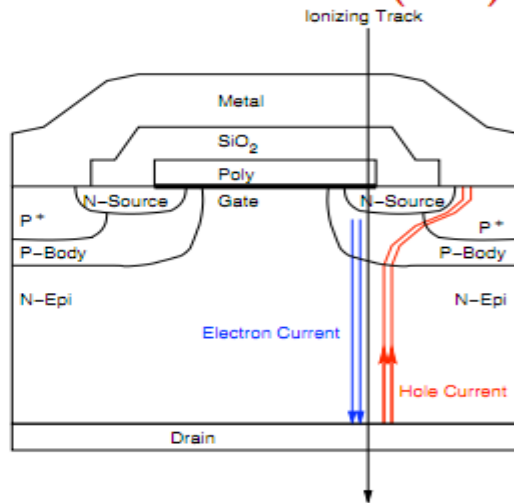


LV Power Supply failures in CDF

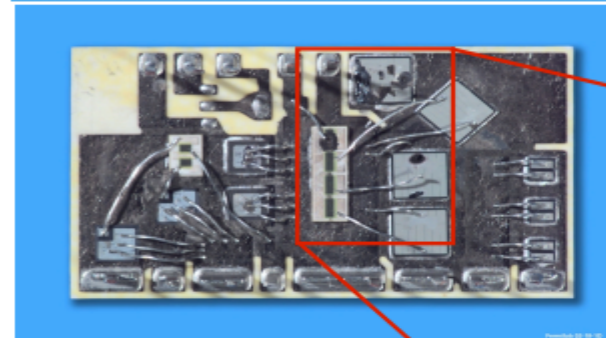
Power Factor Corrector Circuit

Most failures were associated with high beam losses or misaligned beam pipe

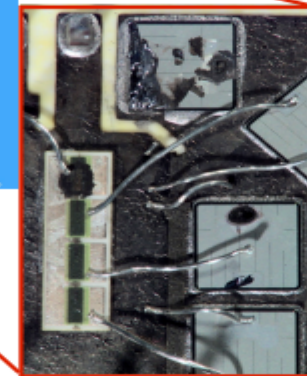
> Power MOSFET Single Event Burnout (SEB)



epoxy covering fractured



silicon in MOSFET sublimated during discharge through single component



as a consequence

CMS developed with CAEN SEB/SEU tolerant power supplies

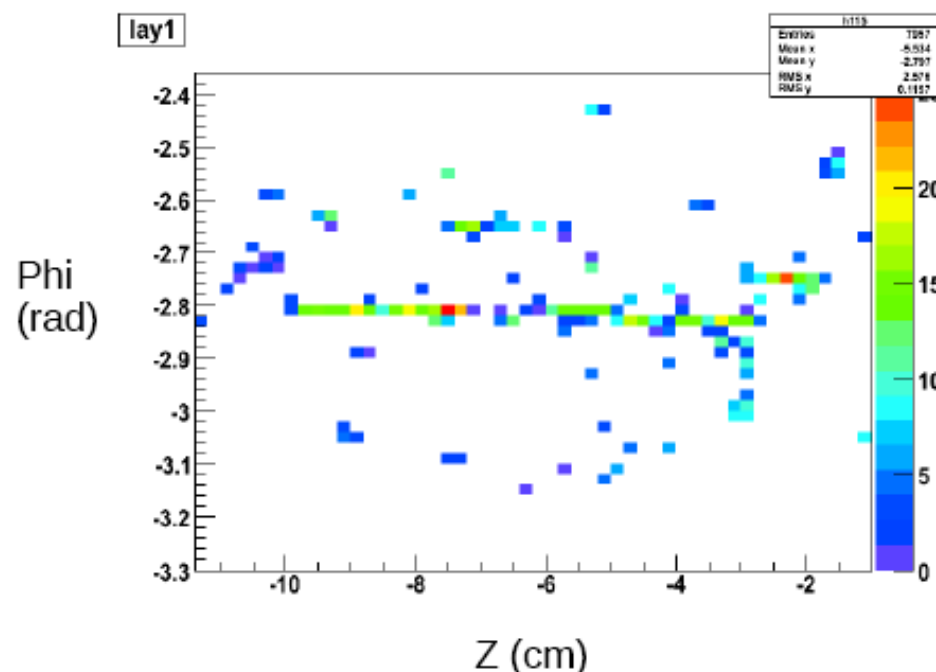


Loss of channels in the vertex detector due to beam incident

- 9 CDF SXV3D chips were damaged in two separate incidents (high inst. Particle flux, 10^7 MIPs/cm² in 150ns)
- Abort magnet switch failure (“kicker pre-fire”)
- Implemented at FNAL:
 - Fast interlock to abort beam when if RF failure occurs before beam is de-bunched
 - Position collimators to intercept deflected particles in the event of kicker pre-fire
- Consequences for CMS
 - Collimation system optimized with detector safety in mind (not just accelerator components)

Pixel detector: Beam gas backgrounds

An event display of a part of
the pixel barrel layer-1 detector



We saw the effect of such events within a few minutes after switching on the pixel detector for the first time with beam in December 2009.

The very large local occupancy keeps the readout channel (FED) busy for a long time. If a next event comes soon after, it might be skipped causing a loss of the event synchronization.

DAQ resets were needed to recover.

The high granularity along the beam line in a pixel detector increase the sensitivity to beam background (beam-gas collisions) events. Beam-gas collision produce tracks that graze along the length of the pixel modules producing large occupancy and long readout time. Such effect can contribute substantially to the experiment dead-time.

summary

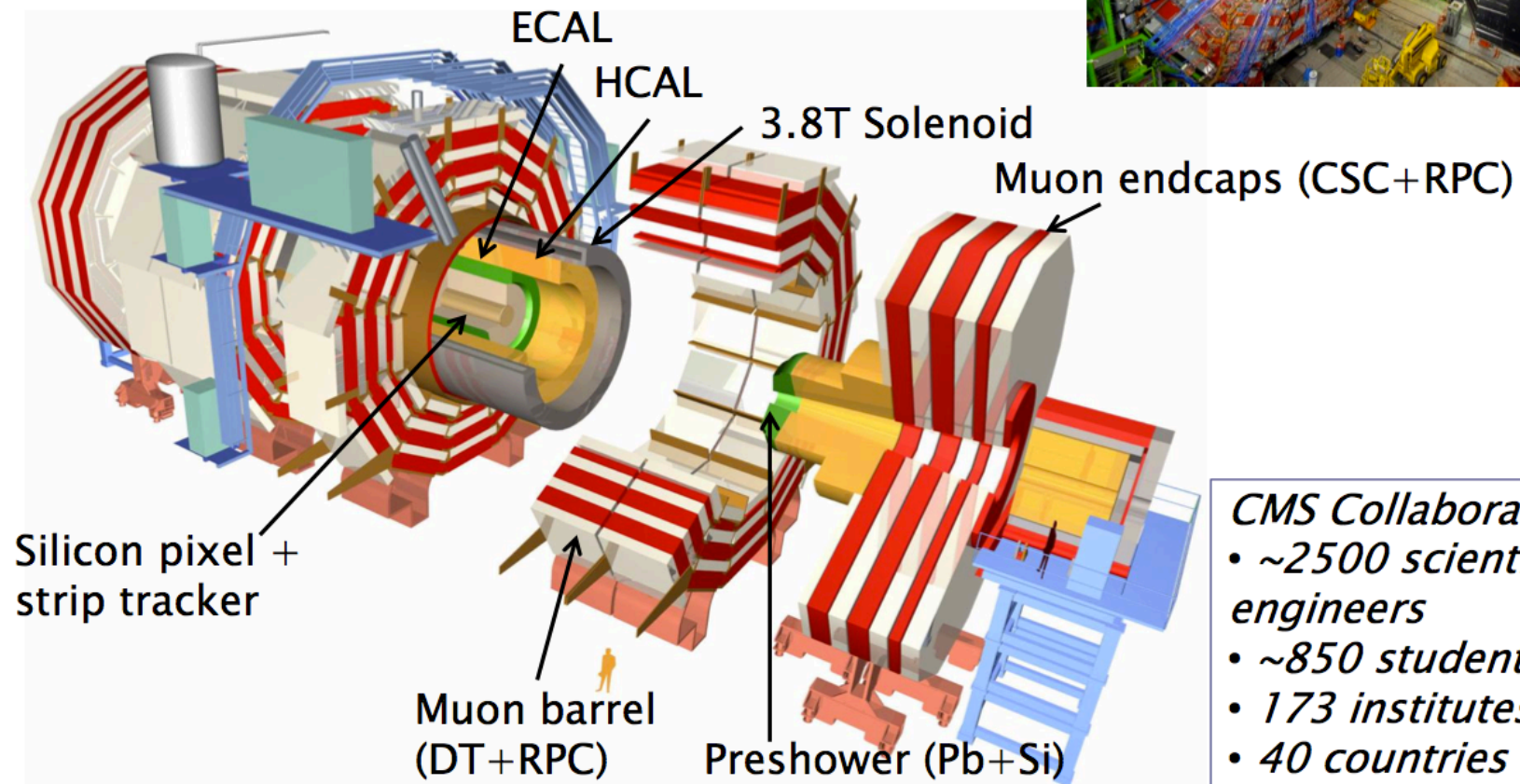
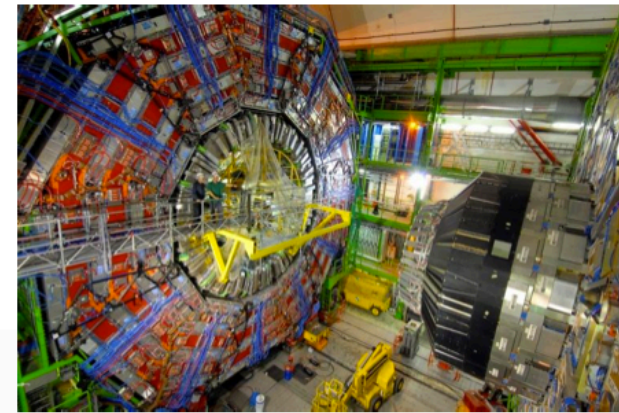
- LHC detectors benefited from experience gained during operation of Tevatron collider
- ATLAS and CMS detectors cope well with new and challenging operational conditions at LHC:
 - 50 ns bunch spacing
 - Hi-pile up
 - Beam related noise
- Upgrade programs are well underway to address known limitations and be ready for further improvements in LHC performance

Back-up

30

The CMS Detector

- 21m long, 15m in diameter
- 12500 tons

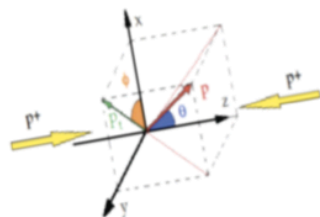


CMS Collaboration:

- ~2500 scientists + engineers
- ~850 students
- 173 institutes
- 40 countries

ATLAS detector

The ATLAS detector

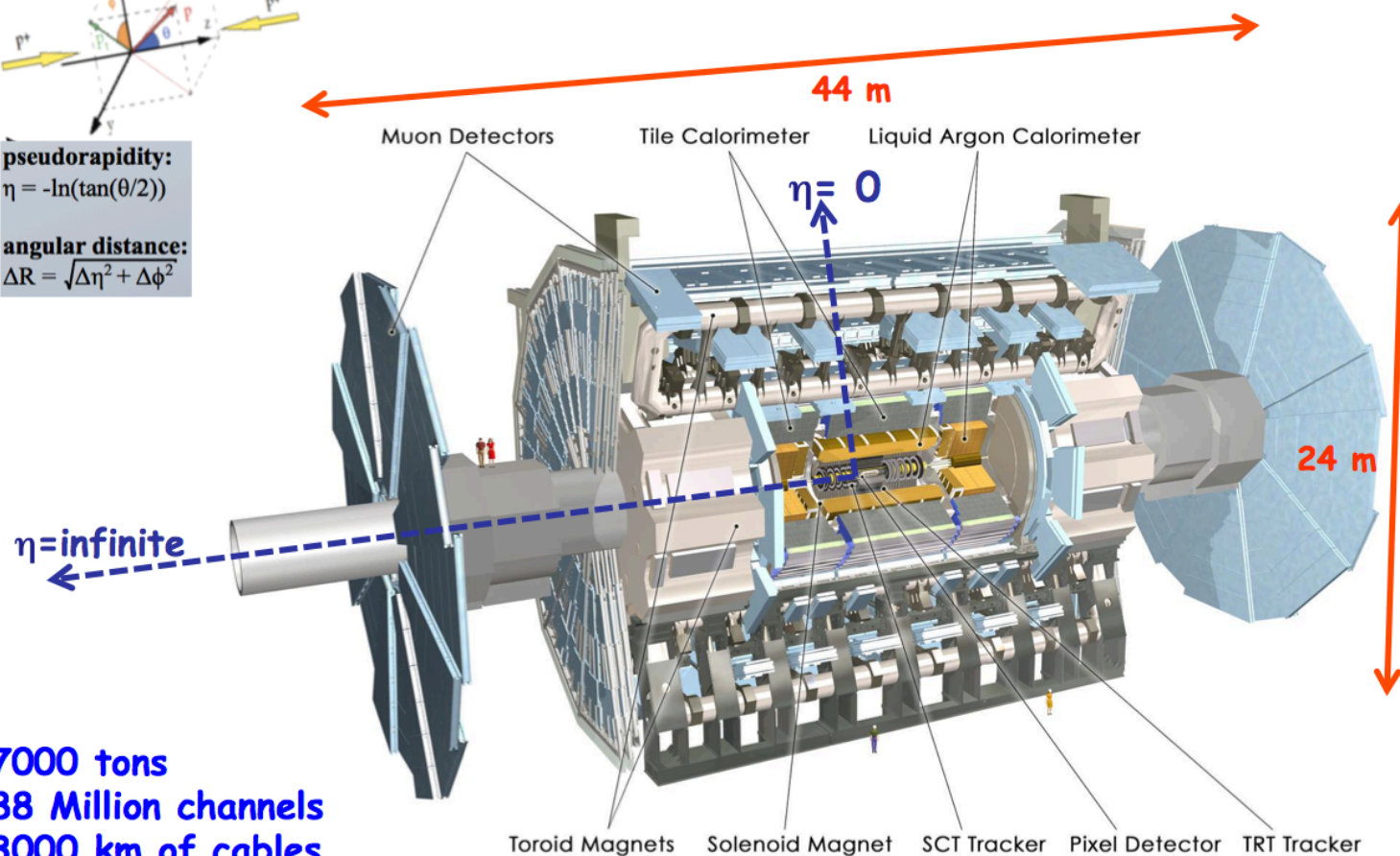


pseudorapidity:

$$\eta = -\ln(\tan(\theta/2))$$

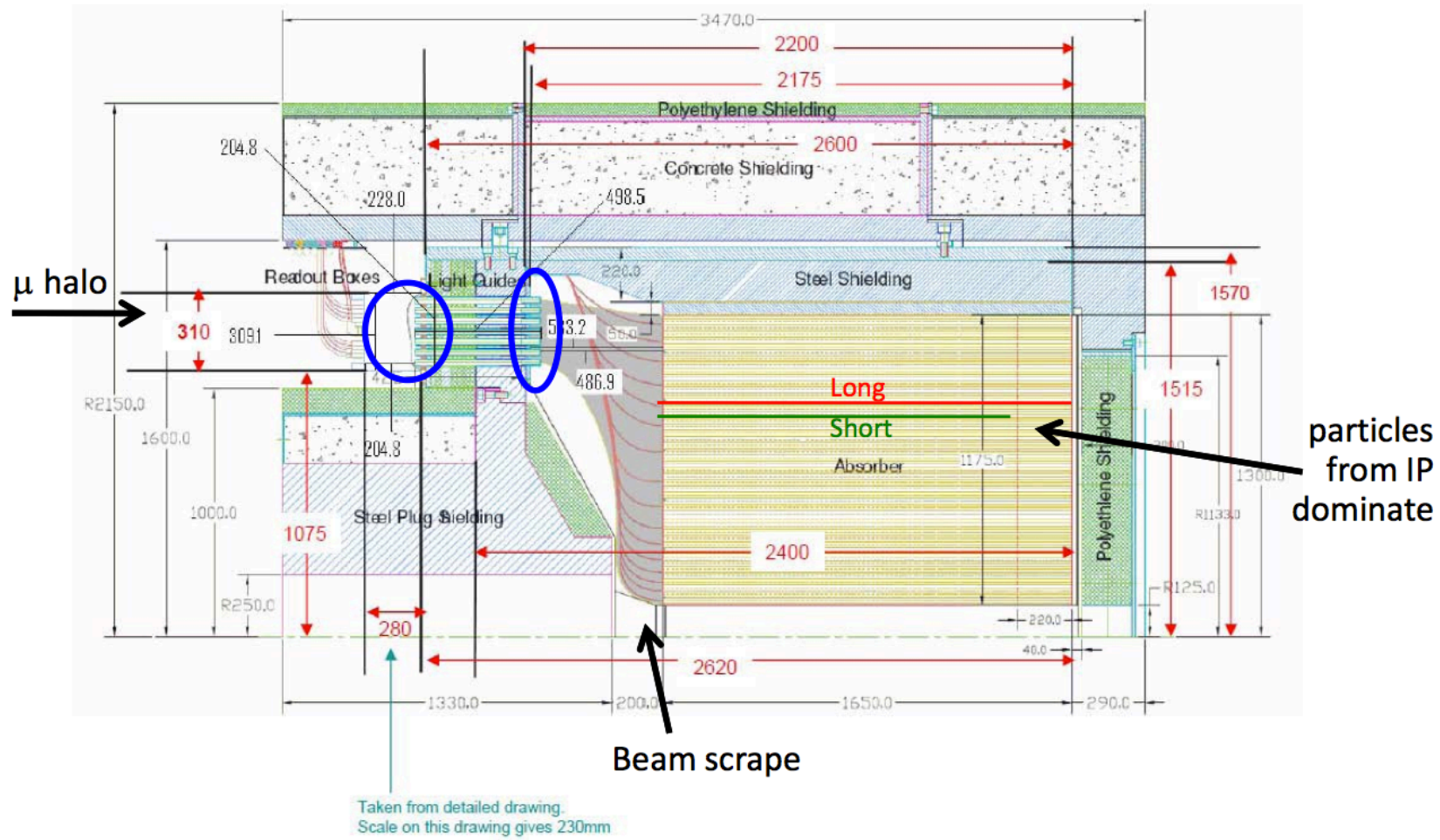
angular distance:

$$\Delta R = \sqrt{\Delta\eta^2 + \Delta\phi^2}$$



7000 tons
 88 Million channels
 3000 km of cables
 2T solenoid
 Toroid ($B \sim 0.5\text{T}$ in barrel; $\sim 1\text{T}$ end-cap)

Possible sources of HF anomalous signals



modifications to reduce noise in HF

34



Oct 2010: removal of scintillating light guide from HPF($\phi=3$)

Jan 2011: installation of non-scintillating sleeves for all HF channels

Apr 2011: enabling of PreBX veto (blocks L1 triggers which come 1BX prior to collisions, as defined by BPTX)

2013 Shutdown: exchange of present HF PMTs for thin window, multi-anode PMTs

R7600U-200-M4



advantages

1. Thin glass reduces the size of window hitting events.
2. Metal envelope reduces window hitting events rate.
3. Multi-anode allows to tag window hitting events.
4. Multi-anode allows to correct window hit energy.
5. High Q.E. and gain improves HF resolution.
6. Meshed structure makes it less susceptible to B Fields.

Batch of 300 PMTs delivered to Iowa, 200 already tested

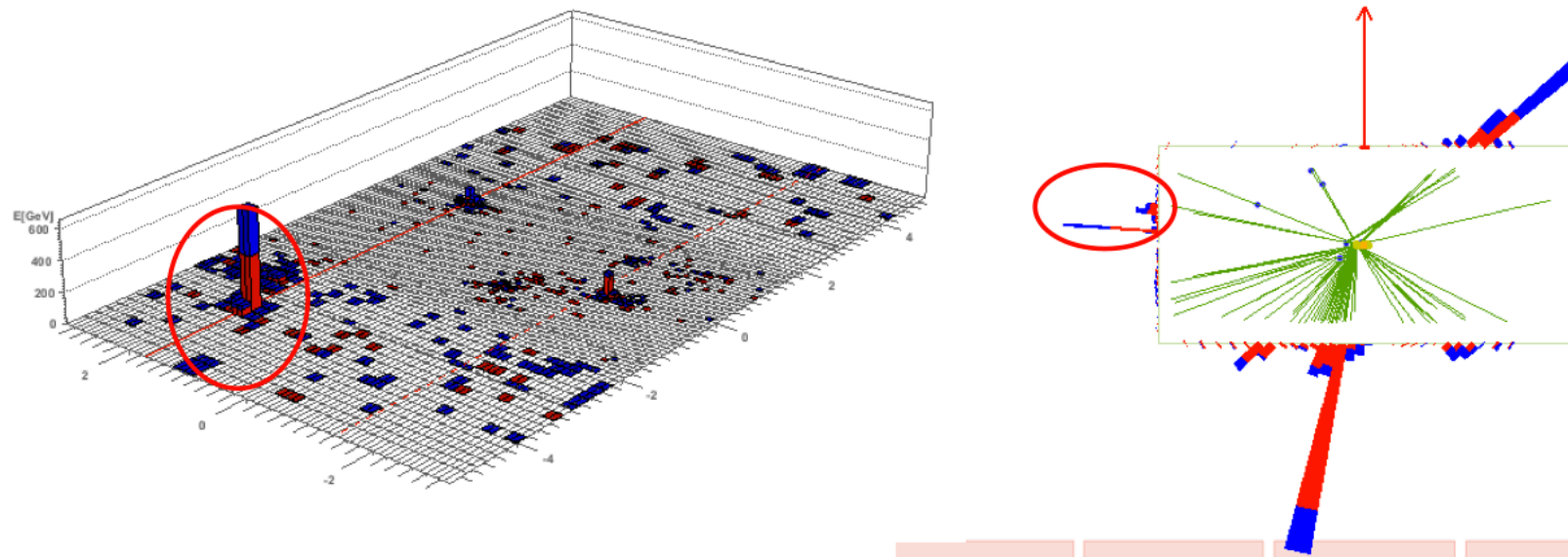
HF residual noise

The HF noise cleaning is very effective, but a residual very low rate of background at high E_T will be difficult to remove.

Appears to be due to late developing showers (the HF absorber is 8.8λ) which punch through into the PMT region producing a cluster of narrow early/in-time hits and sometimes longer “discharge-like” pulses with apparent very high energy.

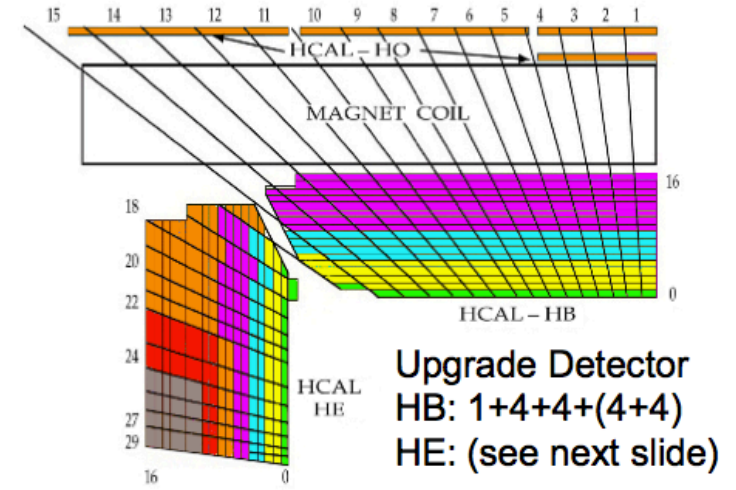
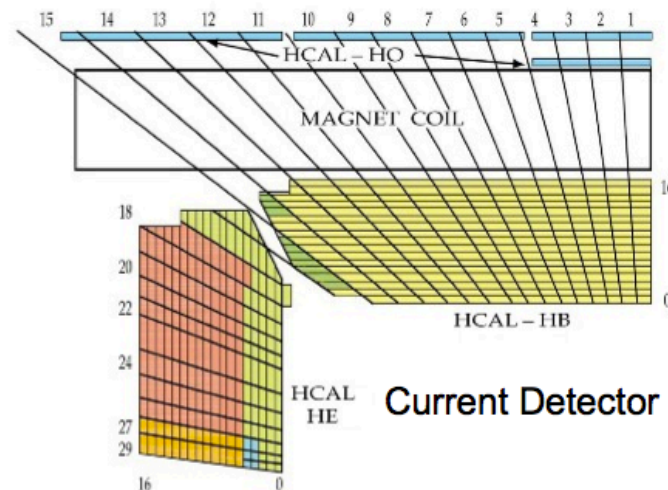
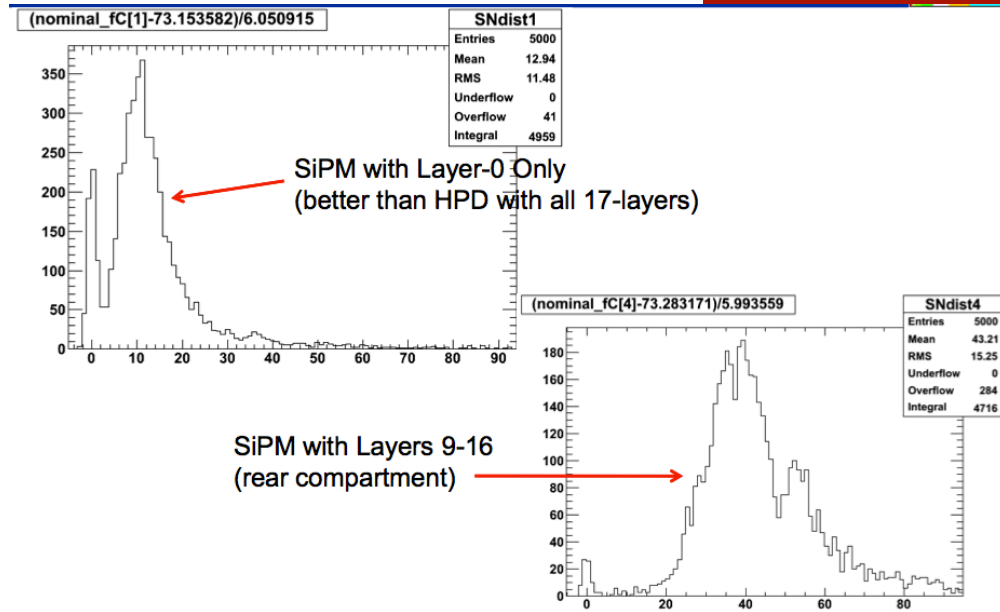
Such multi-hit clusters can be mixed in with “real” event data.

The upgrade PMTs will reduce the rate and provide additional handles.



SiPM performance in Barrel (TB results)

- * In HB, present single-depth readout will be replaced with 4-depths
- * In HE, present 2-3 depth readout will be replaced with 5-depths
- * Final choice (partially driven by technical considerations) to be determined



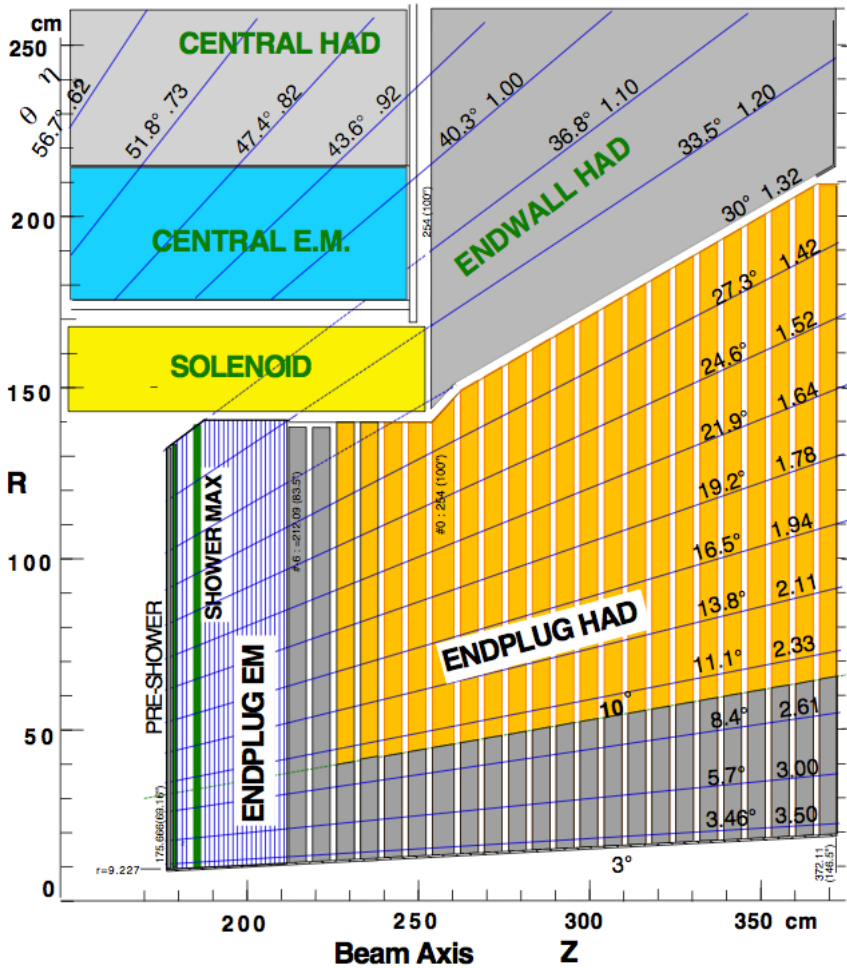
HCAL upgrade activities

HCAL upgrade activities in the period of time between now
and the end of 2nd Long Shutdown of LHC (2018 ?)

- **Present Issues:**
 - HPD discharges (problem in HBHE and HO)
 - PMT background (problem in HF)
- **Photo-detector replacements in 2013-14**
 - HO: Replacement of HPDs with SiPMs
 - HF: Replacement of present PMTs with thin window, multi-anode PMTs
- **Photo-detector replacements in 2018-19**
 - HBHE: Replacement of HPDs with SiPMs
 - it will increase performance,
 - Allow for increased longitudinal/transverse segmentation,
 - add hardware timing
- **Front-end and Back-end upgrade**
 - FE/BE communication and Back-end upgrade
 - it will improve increase robustness of FE/BE communication, upgrade bandwidth into Calorimeter trigger, contribute to improvement of trigger

CDF Plug (= Endcap) Calorimeter

5. Side view of the east end plug, the WHA, and portions of the solenoid, CEM, and CHA



6. PEM and PHA detail summary

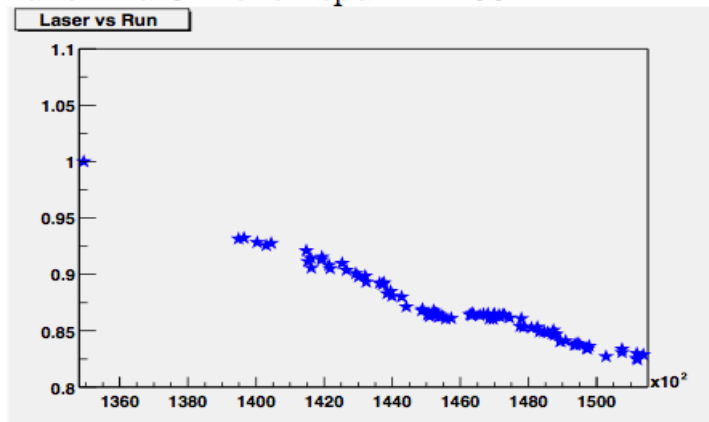
	PEM	PHA
Coverage	$1.1 < \eta < 3.64$	$1.2 < \eta < 3.64$
Towers	20 per wedge	18 per wedge
Thickness	$21 X_0, 1 \lambda_I$	$7 \lambda_I$
Density	$0.36 \rho_{Pb}$	$0.75 \rho_{Fe}$
Sampling Layers	22 + PPR PPR = Layer 1	22
Scintillator	4mm SCSN38	6mm SCSN38
Absorber	4.5mm Pb with 0.5mm SS covers	5.08cm Fe
Light	5 pe/mip/tile 400 pe/GeV	5 pe/mip/tile 40 pe/GeV
Light x-talk	0.5% per side	1.0% per side
σ/E	$0.16/\sqrt{E} \oplus 0.01$	$0.74/\sqrt{E} \oplus 0.04$
PMTs	Hamamatsu R4125	Hamamatsu R4125

- SCSN38: Kuraray polystyrene scintillator
- R4125: 0.75" green extended version of R580
- σ/E from 1996–97 test beam run

CDF Plug PMT gain loss

3. PEM and PHA PMT gain drop

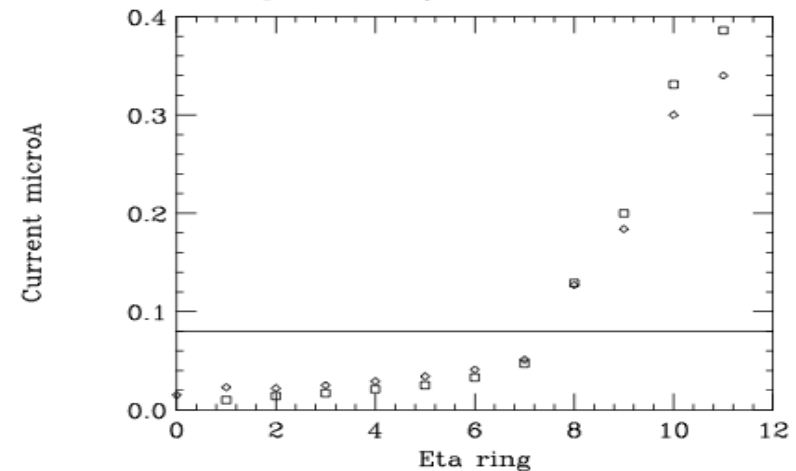
- Or why it is important to take plug laser and radioactive source calibrations
- Big tower gain drops seen in laser calibration runs in a 3 month span in 2002:



Same drop in radioactive source calibrations, so not scintillator aging.

- Sign of PMT aging – decrease in gain with increasing integrated charge
- But: total integrated charge was very small and inconsistent with expectations
- Not seen in PPR or PES

- Effect clearly scales with PMT currents
 - The underlying cause is not understood
 - Clear solution: reduce integrated charge
- Steps to reduce integrated charge on PMTs
 - Shot setup: HV set to standby (60% gain) until scraping complete
 - Data taking: 0.080 μA current limit

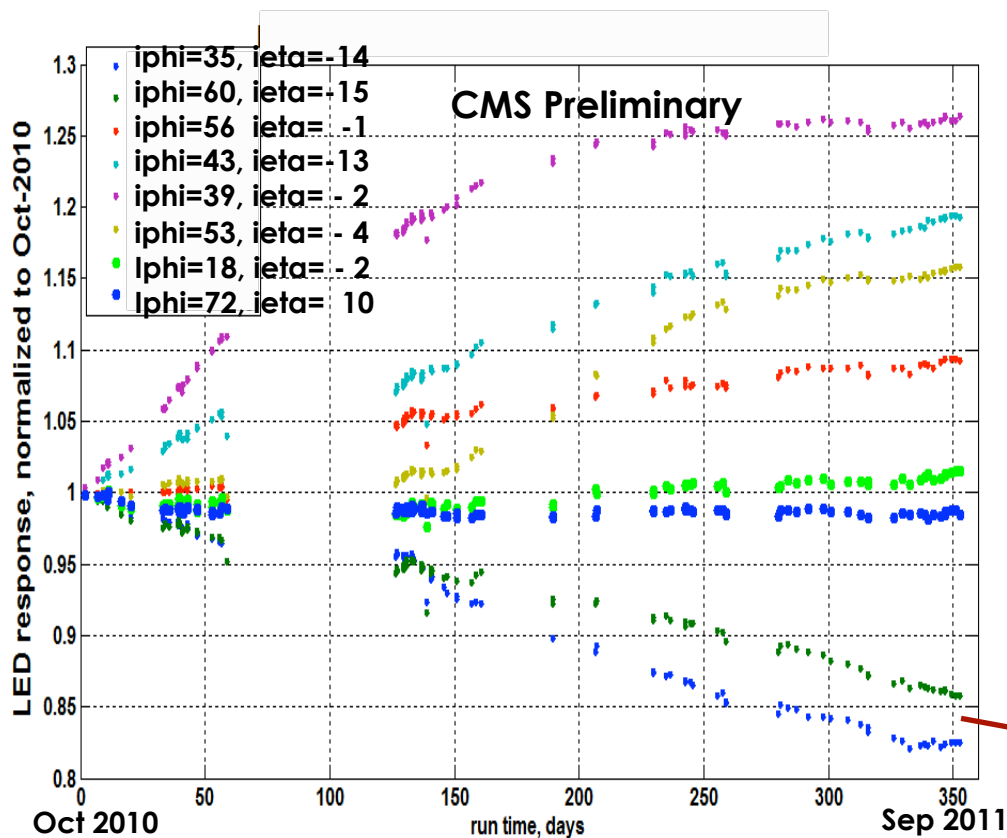


- Lower high η PMT HV
- Compensate loss via software LER gain

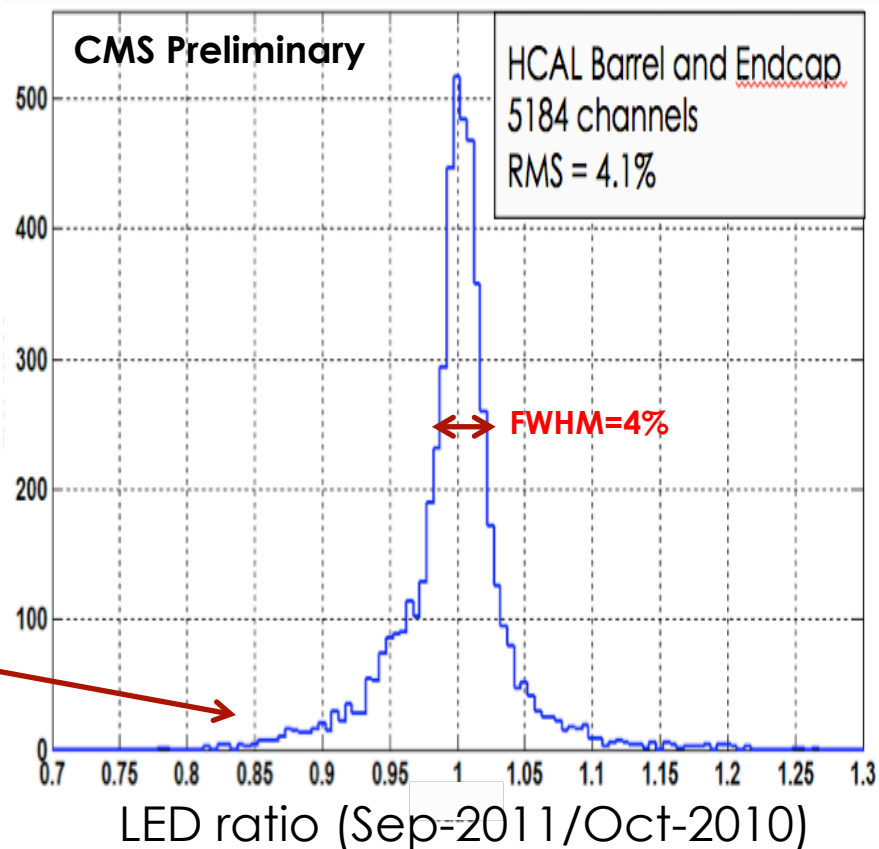
LED Corrections (2011)

HCAL Barrel

Response of selected channels to LED signals vs time



LED gain change corrections, Sep-2011/Oct-2010



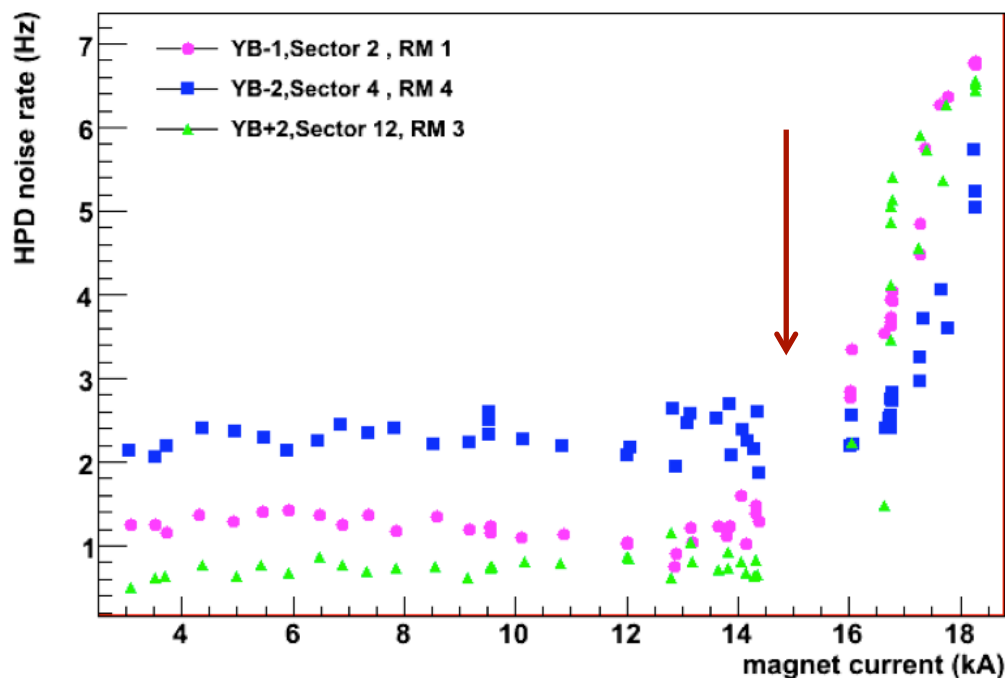
Most of HCAL Barrel and Endcap channels are stable at the level of 2-3% over period of one year. However, approximately 4% of channels exhibit gain drifts $\sim 10\%$ in time period Oct-2010 to Sep-2011. $i\eta$ and $i\phi$ are defined as integer indexes of HCAL Barrel towers in η and ϕ dimensions.

Performance of HO HPDs in CMS magnetic field

- * HPD discharge noise in B field known since 2006
- In 2009, several HPDs replaced to maintain HO operational

CMS@3.8T, B field in HO1,2: $\sim 0.3T$

HO HPD noise rate vs magnet current



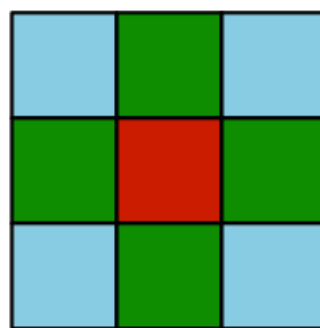
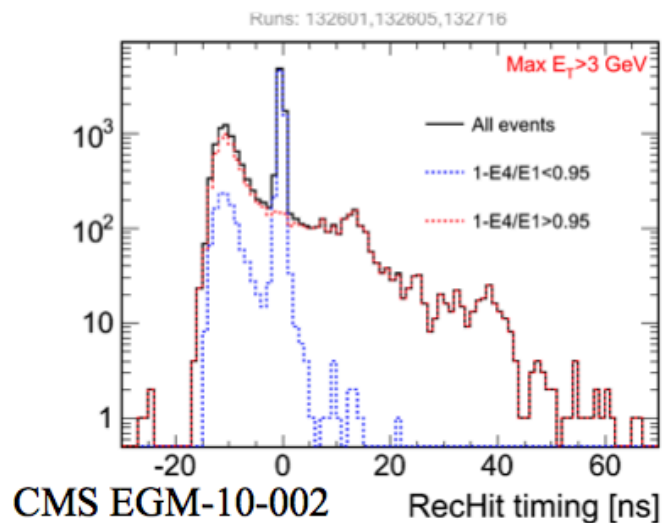
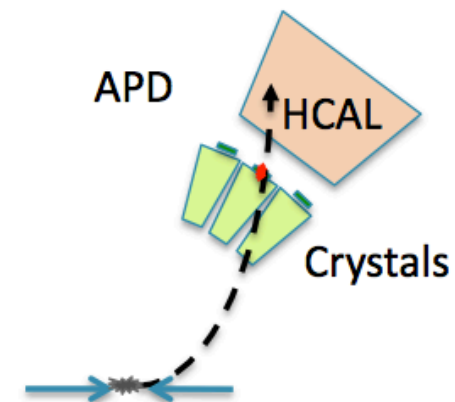
- Noise activity inside HPD at intermediate B-field levels.
- electron avalanches caused on tube walls.
- Problematic in HO area, where B is inhomogeneous and $< 4T$.
- Gain of HPDs (1500 @ 8 kV) is slightly marginal for HO area, where the signal comes only from a 5 mm thick scintillator tile.

CMS ECAL noise:

Anomalous high energy signals in single isolated channels in the barrel have been observed during the collisions. This is due to direct energy deposition in the depleted bulk of an APD.

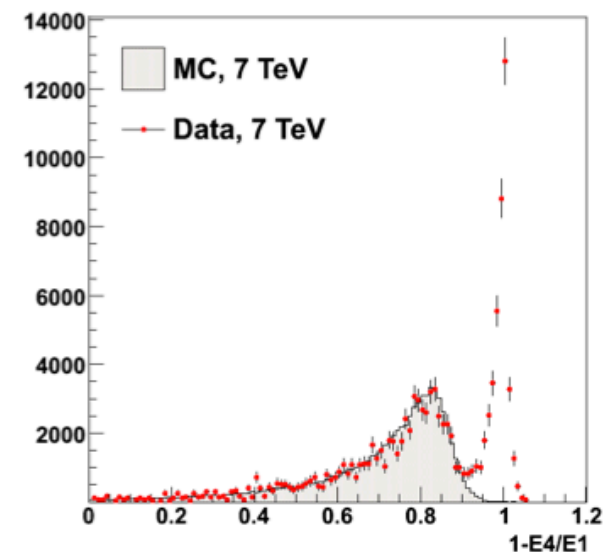
They can be identified with:

- topological selection \rightarrow isolated channels
- different timing
- differences in the pulse shape



For anomalous signals

$$1 - E_4/E_1 \sim 1$$



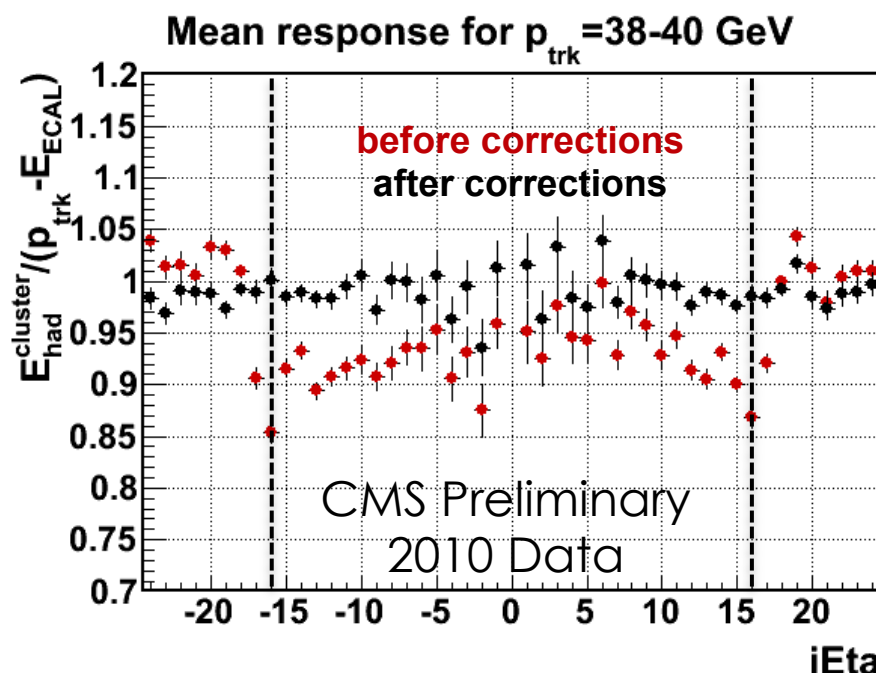
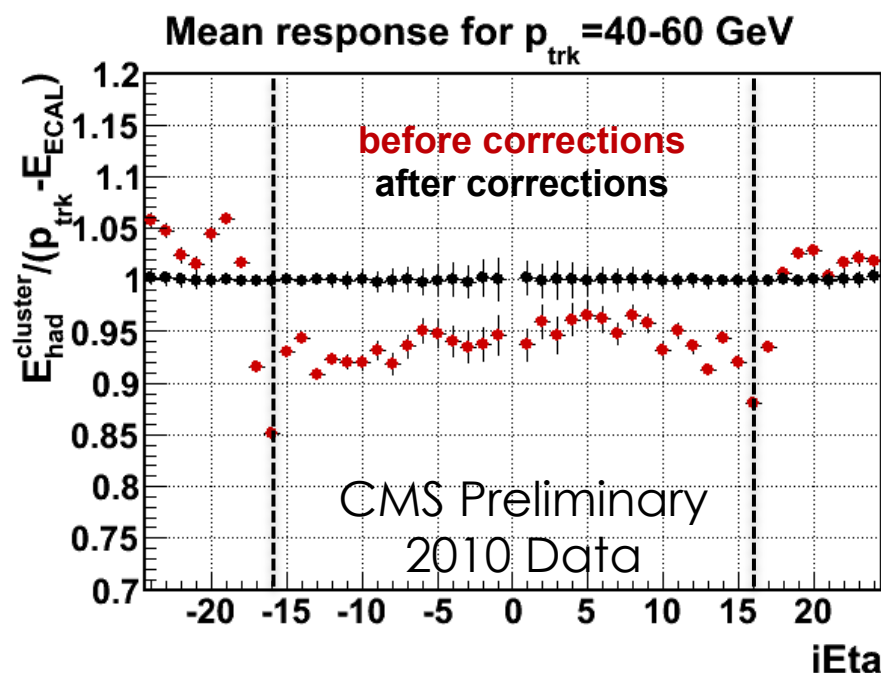
Isolated Hadron Response in 2010 Data

Isolated tracks used to apply an eta-dependent energy correction to the data up to $|\eta| \leq 22$, $|\eta| < 2.4$

Dedicated trigger selecting events with isolated tracks with $P_T > 38 \text{ GeV}$

Derive corrections using $p_{\text{trk}} = 40\text{-}60 \text{ GeV}$

Check method using lower p_{trk} tracks



Dashed lines indicate the last η -ring of HCAL barrel detector ($|\eta| = 1.4$)